nature communications

Article

https://doi.org/10.1038/s41467-026-69008-9

The focal adhesion kinases regulate leptin action and the weight reducing effect of HDAC6 inhibition

Received: 15 September 2023

Accepted: 22 January 2026

Published online: 05 February 2026

Check for updates

Colleen K. Hadley[1,2,3,9], Luca Galgano[1,4,5,6,9], Yijun Gui[1,7,9], Antonio M. Carvalho da Silva[1,9], Danielle T. Porter[1], Yanan Wu[1,7], Yuanting Lai[6,8], Mauro Torti[4] & Işın Çakır[1,6]

The adipokine leptin is a central regulator of energy metabolism. We previously showed that HDAC6 inhibitors enhance central leptin sensitivity. Using integrative analyses of leptin-responsive hypothalamic gene expression signatures, we identified focal adhesion kinases (FAK and PYK2) as essential for the anorectic effect of leptin and the anti-obesity action of HDAC6 inhibitors in male mice. The effect of tubastatin A, an HDAC6 inhibitor, is compromised in Pyk2 knockout mice, and central inhibition of focal adhesion kinases blocks tubastatin-induced weight loss. Focal adhesion kinases phosphorylate and activate the transcription factor STAT3 downstream of leptin receptor, and leptin signaling is attenuated when these kinases are knocked down or inhibited. Finally, hypothalamic knockdown of focal adhesion kinases blunts leptin action, leads to hyperphagic obesity, and attenuates the anti-obesity effect of HDAC6 inhibitors. These findings suggest that FAK and PYK2 are previously uncharacterized members of the leptin receptor signaling and critical mediators of central leptin sensitization.

The adipose-derived hormone leptin is secreted in amounts proportional to adiposity. In mammals, leptin exerts an anorectic effect and suppresses food intake upon peripheral or central administration[1,2]. In humans and rodents, mutations in the gene encoding leptin or its receptor result in profound hyperphagia, severe obesity, hyperglycemia, and impaired endocrine functions, emphasizing the critical contribution of leptin to the maintenance of energy balance[3,4].

The effect of leptin on energy homeostasis is predominantly mediated through neurons expressing the long isoform of the leptin receptor (LepRb) within the central nervous system[5,6]. Binding of leptin to LepRb stimulates several intracellular signal transduction mechanisms including the janus kinase 2 (JAK2)/signal transducer and activator of transcription 3 (STAT3) pathway. Upon LepRb activation, JAK2 is recruited and phosphorylates the intracellular tyrosine residues of LepRb, leading to the recruitment of STAT3. JAK2 phosphorylation of STAT3 tyrosine residue 705 ($pSTAT3^{Y705}$) promotes dimerization of STAT3 and its subsequent nuclear translocation. STAT3 expression in LepRb neurons is required for the leptin-dependent regulation of energy balance, emphasizing the dominant contribution of STAT3-dependent signal transduction over other pathways activated by leptin[7–9]. JAK2, however, is not required for the activation of STAT3 in response to leptin in vitro[10], suggesting that other tyrosine kinases may be involved in mediating this action. Notably, STAT3 is an established target of focal adhesion kinases[11–13],

[1]Life Sciences Institute, University of Michigan, Ann Arbor, MI, USA. [2]College of Literature, Science, and the Arts, University of Michigan, Ann Arbor, MI, USA. [3]Weill Cornell/Rockefeller/Sloan Kettering Tri-institutional MD-PhD Program, New York, NY, USA. [4]Department of Biology and Biotechnology, University of Pavia, Pavia, Italy. [5]Scuola Universitaria Superiore, IUSS, Pavia, Italy. [6]Division of Endocrinology and Metabolism, Department of Medicine, University of Pittsburgh, Pittsburgh, PA, USA. [7]Department of Molecular, Cellular and Developmental Biology, University of Michigan, Ann Arbor, MI, USA. [8]State Key Laboratory of Genetic Engineering, School of Life Sciences, Fudan University, Shanghai, China. [9]These authors contributed equally: Colleen K. Hadley, Luca Galgano, Yijun Gui, Antonio M. Carvalho da Silva. e-mail: cakiri@pitt.edu

however whether focal adhesion kinase (FAK) and protein tyrosine kinase 2b (PYK2) regulate leptin action is unknown.

FAK and PYK2 comprise the focal adhesion kinase family, a subset of non-receptor tyrosine kinases with 46% sequence identity and 65% amino acid similarity[14]. The focal adhesion kinases play a key role in several cell activities due to their interaction with the cytoskeleton and activation by integrins and G-protein coupled receptors[15,16]. While FAK is ubiquitously expressed, PYK2 expression is primarily limited to the CNS and cells of hematopoietic lineage, although PYK2 is also expressed in other cell types[17,18]. Pyk2 knockout (KO) mice are viable and fertile[19], however *Fak* ablation leads to early embryonic lethality because of defects in vasculogenesis[20,21], although the knockdown of *Fak* expression in some tissues (e.g., endothelium) is compensated with elevated PYK2 expression[22–25]. While both proteins regulate cell motility and migration, polarization, adhesion, and proliferation[16,19,26–31], PYK2 is also involved in spatial memory and synaptic plasticity, synaptic remodeling[32–35], and signal transduction in response to cytokine and growth factor receptor activation[36–39].

The focal adhesion kinases have also been implicated in metabolism. Modest knockdown of *Fak* in the muscle and liver of lean wild-type mice results in increased food intake and body weight and impaired insulin sensitivity[40]. Furthermore, adipocyte FAK is necessary for cell survival and insulin sensitivity in the obese state. Consequently, HFD-induced obese mice with an adipose tissue-specific deletion of *Fak* exhibit greater impairments in obesity-induced insulin sensitivity[41]. Pyk2 KO mice were reported to be more prone to obesity and exhibit exacerbated obesity-associated impairments in glucose homeostasis[42]. The metabolic deficits associated with the tissue specific *Fak* and whole-body Pyk2 KO mouse models suggest a role for the focal adhesion kinases in the regulation of energy homeostasis. The precise pathway(s) and mechanism(s) by which the focal adhesion kinases regulate energy homeostasis, especially in the context of their central action, remains largely unknown. Furthermore, their potential role in hypothalamic leptin receptor signaling has not been studied.

In diet-induced obese (DIO) rodents and humans, circulating leptin concentrations rise in proportion to adiposity. This hyperleptinemic state is causally linked to the development of leptin resistance[43]. Our group has recently identified that peripheral, but not central, inhibition of HDAC6 activity leads to central leptin sensitization through a systemic factor[44]. Furthermore, inhibition of endogenous HDAC6 in LepRb-expressing cells does not alter leptin action[44]. Small molecule HDAC6 inhibitors act as a potent leptin-sensitizers and anti-obesity agents, however the central mediators of these actions are unknown.

Here, we show that focal adhesion kinases are required for the anorectic action of leptin and the anti-obesity effect of HDAC6 inhibitors. FAK and PYK2 physically interact with and phosphorylate STAT3 in response to leptin. Accordingly, pharmacological or genetic inhibition of focal adhesion kinases attenuate leptin signaling. AAV-mediated knockdown of these kinases in the hypothalamus of lean mice results in hyperphagic obesity and resistance to the weight reducing effect of HDAC6 inhibitors. Our results suggest focal adhesion kinases as new regulators of leptin receptor signaling and thus critical components of the homeostatic body weight regulation.

Results

DIO mice treated systemically with HDAC6 inhibitors, including Tubastatin A (TubA), regain their hypothalamic leptin sensitivity and lose weight[44]. However the central mechanism of action of this leptin sensitization is unclear[44,45]. To discover genetic and/or pharmacological interventions with effects on gene expression resembling the hypothalamic transcriptomic signatures of leptin sensitization, we utilized Connectivity Map (CMap, clue.io), a database of transcriptomic profiles of human cells subjected to thousands of perturbagens; small molecule compounds or genetic manipulations (overexpression and/or knock-down). To this end, we first used the hypothalamic transcriptome in response to systemic TubA administration in obese mice, as this represents a leptin sensitized state (Fig. 1a and Supplementary Data 1), to query the Connectivity Map (CMap) database (detailed in the "Methods"). Since leptin receptor expressing neurons constitute a small percentage of the total hypothalamic cell pool, we also gathered the leptin regulated and LepR$^+$ neuron-enriched gene lists[46] (Fig. 1c), and conducted an independent CMap search with the differentially expressed gene set representing leptin's signature (differentially expressed genes in LepR+ neurons), Fig. 1d). CMap queries with either input resulted in a set of compounds and genetic perturbations that partially overlapped (Fig. 1b, d and Supplementary Data 2). To narrow down candidate factors that mediate central leptin sensitization conferred by HDAC6 inhibition, we combined the two lists by averaging their connectivity scores (Fig. 1e, f). Based on subsequent analysis of the final candidate list (see "Methods"), we prioritized focal adhesion kinases for further investigation for the following reasons: The compound, PF-562271, which is a dual focal adhesion kinase inhibitor, was the second most significantly and negatively correlated perturbagen when the TubA and leptin signatures were co-analyzed (Fig. 1f). *Pyk2*, one of the two focal adhesion kinases, was highly upregulated in the hypothalamic of TubA-treated mice (Fig. 1a), and TubA treatment also increased the hypothalamic *Fak* expression in DIO animals (1.00 ± 0.06 vs. 1.34 ± 0.09 for vehicle vs. TubA, respectively, $p = 0.018$). Furthermore, *Pyk2* is significantly associated with body mass index (BMI) and weight in human genome-wide association studies with a Human Genetic Evidence[47,48] score of 45 (very strong) (Supplementary Fig. 1a, b). Likewise, *Fak*, the other focal adhesion kinase, is linked to waist-hip ratio and cardiovascular traits such as blood pressure and elevated cholesterol (Supplementary Fig. 1c, d), collectively suggesting that focal adhesion kinases could be involved in the central regulation of energy balance.

FAK and PYK2 mediate the weight reducing effect of TubA

We next set to determine if focal adhesion kinases are required for TubA-induced weight loss. We first tested the effect of dual central inhibition of the focal adhesion kinases on TubA action using PF-431396 (PF), an ATP-mimetic highly selective dual inhibitor of FAK and PYK2[49]. Following daily central infusion of vehicle or PF to DIO wild-type mice, we treated mice with peripheral injection of vehicle or TubA (15 mg/kg) for five consecutive days. Of note, at this dose, TubA reduces obesity in DIO wild-type mice but not in HDAC6 KO animals[44]. TubA treatment led to a steady weight loss in DIO mice during the treatment period (Fig. 2a, b and Supplementary Fig. 2a). However, central PF infusion conferred significant resistance to TubA-induced weight loss (Fig. 2a, b).

The PF compound is a dual inhibitor of both FAK and PYK2. Since whole body *Fak* deletion leads to embryonic lethality, but Pyk2 KO mice develop normally, we tested if Pyk2 KO mice exhibited resistance to TubA. We induced obesity by feeding Pyk2 KO mice and their wild-type littermates HFD for 24 weeks. In contrast to a previous study[42], Pyk2 KOs displayed similar weight gain and food intake on HFD when compared to wild-type counterparts (Fig. 2c, d), suggesting that embryonic *Pyk2* ablation alone does not alter the long term energy metabolism of the animals. Following vehicle acclimation, we treated mice with TubA by daily ip injections. While both groups initially started losing weight, Pyk2 KO mice displayed resistance to TubA treatment and their body weight plateaued after the fifth day of the drug administration (Fig. 2e and Supplementary Fig. 2b). During the approximately 2-week treatment period, the TubA-induced weight loss in DIO mice was almost twice as much as that observed in the Pyk2 KO mice (9.98% ± 0.78 vs. 5.40% ± 1.43, mean ± SEM in wild-type vs. Pyk2 KO mice, respectively, $p = 0.0018$) (Fig. 2f). The food intake of the cohorts was comparable during the acclimation phase (Fig. 2g). However, DIO Pyk2 KO mice displayed resistance to the food intake

https://doi.org/10.1038/s41467-026-69008-9

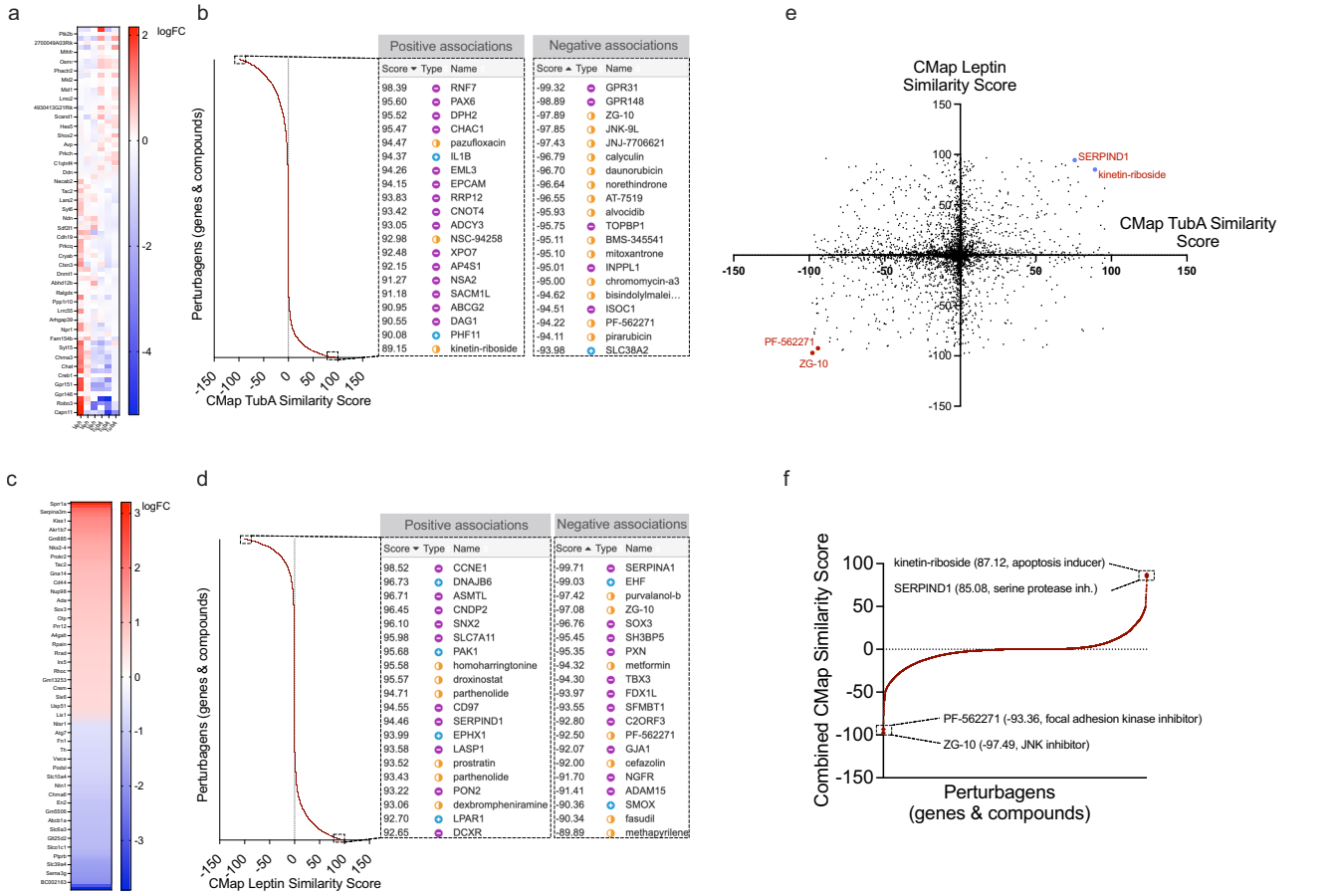

Fig. 1 | Identification of focal adhesion kinases as potential mediators of leptin action and TubA's obesity reducing effect. a Heat map of differentially regulated transcripts obtained by bulk RNA sequencing of the hypothalamic from the DIO wild-type mice treated with vehicle or TubA for four consecutive days ($n = 3$ Veh/TubA mice). **b** Connectivity Map (CMap) similarity scores of the perturbagens for the up- and down-regulated hypothalamic transcripts from TubA-treated mice used as query. Top 20 positively (left) and negatively (right) associated perturbagens are shown. **c** Heat maps of the differentially regulated genes from LepR+ cells obtained from lean wild-type mice after PBS or leptin treatment[46]. **d** CMap scores of the perturbagens and the top associations for the leptin gene expression signature from (**c**). Individual (**e**) and averaged-combined (**f**) CMap similarity scores of TubA and leptin plotted. Top two positively associated and top two negatively associated perturbagens are marked.

suppressing effect of TubA, and the wild-type mice consumed less food under TubA treatment (Fig. 2h, i). While the blood glucose of either group decreased following TubA treatments (Fig. 2j), the decrease in the wild-type mice was more pronounced and significantly more than observed in the Pyk2 KO animals (Fig. 2k). Since Pyk2 deletion conferred a partial resistance to TubA-induced weight loss compared to the more robust resistance by dual inhibition of FAK and PYK2, these results collectively suggest that the central action of focal adhesion kinases is required for the anti-obesity effect of TubA.

FAK and PYK2 are required for leptin-induced STAT3 activation

Because TubA action requires leptin signaling, we next tested if focal adhesion kinases act downstream of leptin receptor. FAK and PYK2 are tyrosine kinases. While JAK2 is the canonical kinase that phosphorylates and activates STAT3, JAK2-independent leptin-STAT3 signaling routes have been reported[10]. To first confirm that JAK2 is not required for the activation of STAT3 by leptin, we assessed STAT3 phosphorylation (pSTAT3^{Y705}) in response to leptin in two independent JAK2-deficient and stably LepRb expressing cell lines, mouse embryonic fibroblasts derived from JAK2 KO mice (MEF JAK2$^{-/-}$)[50] and a human fibroblast cell line genetically deficient of JAK2 (γ2a)[51,52]. Stimulation of LepRb-expressing JAK2$^{-/-}$ MEFs or γ2a cells resulted in the activation of STAT3 in a dose and time-dependent manner (Supplementary Fig. 3a–d). In both cell lines we observed acute activation of STAT3 within 5 min of leptin stimulation (Supplementary Fig. 3c, d). We also observed a second phase of STAT3 activation after 90 min following the initial leptin stimulation in the γ2a cells (Supplementary Fig. 3d). While such a biphasic activation of STAT3 in response to leptin was previously reported[53–55], our results demonstrate that this effect is JAK2 independent. Collectively, these results suggest, consistent with previous reports[10], that JAK2-independent, STAT3-dependent leptin signaling mechanisms exist in vitro, implicating the role of other tyrosine kinases in leptin receptor signaling.

Since both FAK and PYK2 have previously been shown to interact with STAT3[36,56] we tested the focal adhesion kinase family as candidate tyrosine kinases involved in STAT3-dependent leptin action. To determine if either of the focal adhesion kinases activate STAT3, we co-overexpressed STAT3 with either FAK or PYK2 in HEK-293T cells. Both FAK and PYK2 stimulated STAT3 phosphorylation (Fig. 3a, b). Overexpression of the kinase dead (KD) *Fak* or *Pyk2* constructs substantially reduced this effect, suggesting that the catalytic activity of the kinases is necessary for STAT3 activation (Fig. 3a, b). STAT3 co-immunoprecipitated with both PYK2 and FAK in vitro (Fig. 3c) and in the hypothalamic lysates from lean wild-type mice (Fig. 3d). Notably, this interaction was stimulated by leptin in vivo (Fig. 3d), collectively suggesting that both kinases directly interact with STAT3 to promote its activation.

https://doi.org/10.1038/s41467-026-69008-9

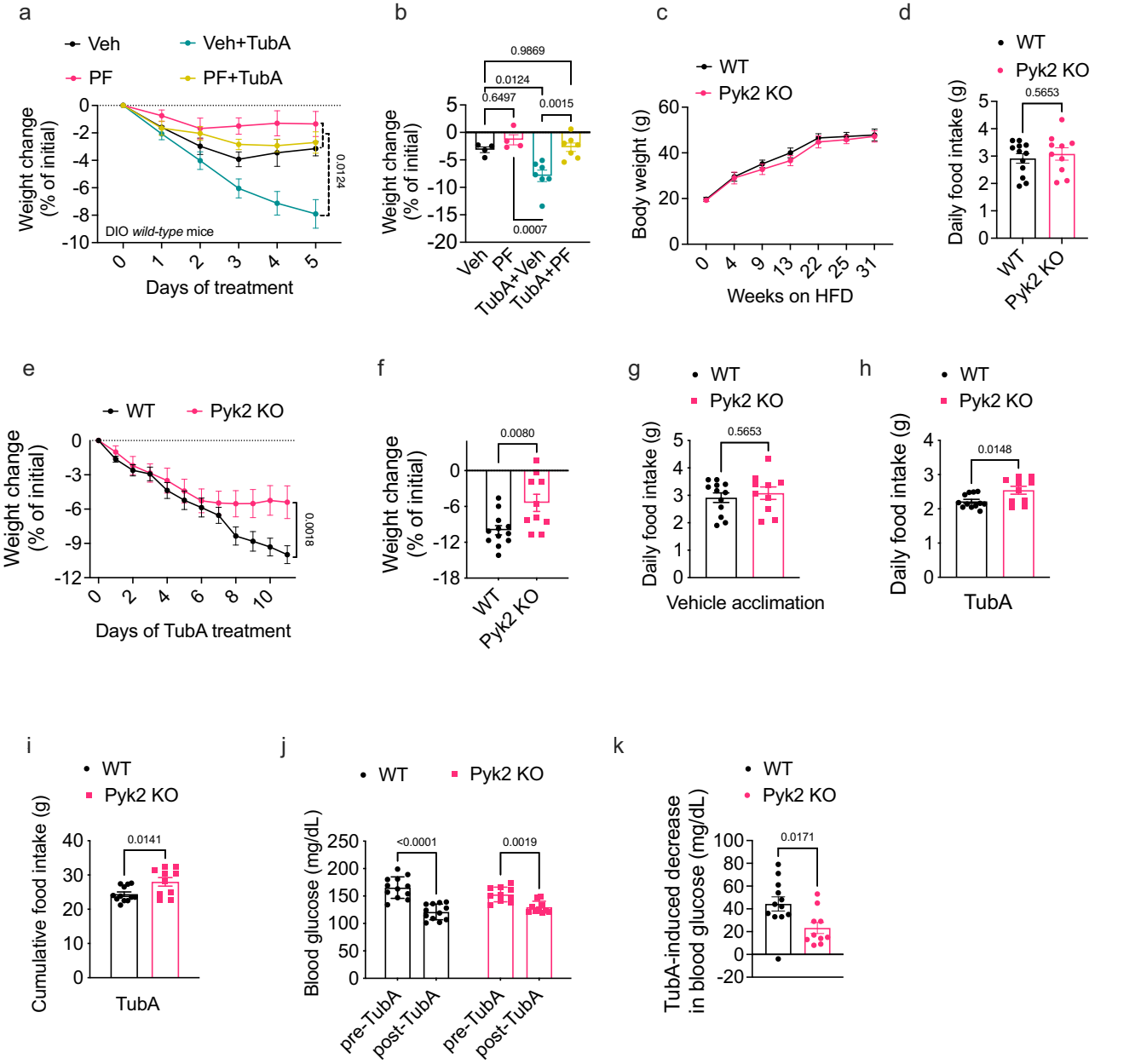

Fig. 2 | PYK2 is required for the anti-obesity effect of TubA. a, **b** DIO wild-type mice that have been on HFD diet were implanted a guide cannula into the lateral ventricle. Mice were treated with vehicle or PF centrally (icv), and vehicle or TubA (15 mg/kg) was administered peripherally once daily. The daily weight change curves (**a**) and cumulative weight change at the end of the treatment (**b**) ($n = 4$ Veh/PF mice; $n = 7$ Veh/PF + TubA mice). **c** Growth curves and **d** average food intake of wild-type or Pyk2 KO mice on HFD. Body weight change of wild-type and Pyk2 KO DIO mice during (**e**) and at the end of (**f**) daily TubA treatments. Average food intake of the animals during vehicle acclimation (**g**) and TubA treatments (**h**). **i** Cumulative food intake of the wild-type and Pyk2 KO mice at the end of TubA treatments. **j** Blood glucose of the mice before and after TubA treatments. **k** Difference in the blood glucose of the mice following TubA treatment ($n = 6$ WT mice; $n = 5$ Pyk2 KO mice). Data shown are representative of experiments conducted once (**a**–**d**) or twice (**e**–**k**) in separate cohorts of animals with similar results. Data are represented as mean ± SEM and analyzed by *t*-test (**d**, **f**–**i**, **k**), mixed effect analysis (**a**), one-way ANOVA (**b**), two-way ANOVA (**c**, **e**, **j**).

We next evaluated if the focal adhesion kinases were required for leptin-induced activation of STAT3. To this end, we used the immortalized mouse hypothalamic N1-LepRb cells, which endogenously express both focal adhesion kinases[44]. Knockdown of either *Fak* or *Pyk2* (Fig. 3e–h and Supplementary Fig. 3e–h), or their dual knockdown (Fig. 3i) resulted in a significant attenuation of leptin-induced STAT3 phosphorylation. Knockdown of either kinase was sufficient to attenuate, but not completely impair, the duration and fold induction of STAT3 activation in response to leptin, and a more robust inhibition of leptin signaling was achieved by dual knockdown of *Fak* and *Pyk2*.

To see if the results from the knockdown studies can be mimicked by the pharmacological inhibition of FAK and PYK2, we tested if PF also impairs STAT3-dependent transcriptional activation. We used a luciferase construct under the transcriptional control of a STAT3 response element such that expression of luciferase is proportional to the transcriptional activity of STAT3[44]. Stimulation of N1-LepRb cells

https://doi.org/10.1038/s41467-026-69008-9

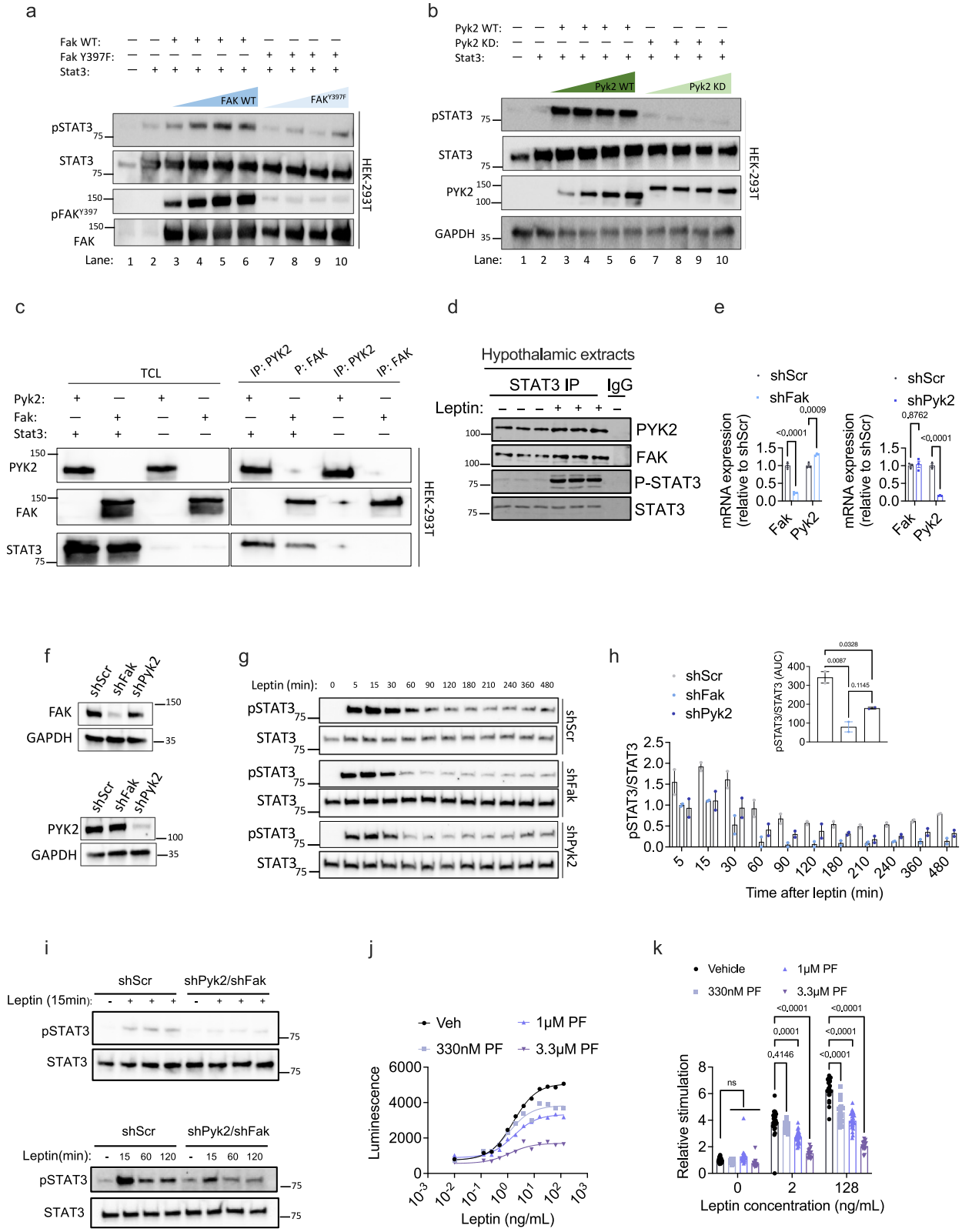

expressing the STAT3-dependent luciferase construct (N1Stat3Luc-LepRb) with leptin for 24 h dose-dependently increased the luminescence (Fig. 3j, k). Treatment of N1Stat3Luc-LepRb cells with PF, however, dose dependently attenuated leptin induced luciferase expression (Fig. 3j, k). We next utilized the γ2a and MEF JAK2$^{-/-}$ cell lines to examine if the result we observed in N1 cells was restricted to a single cell line, and to control for the potential off-target effects of the PF compound on JAK2. Pre-treatment of stably LepRb-expressing JAK2$^{-/-}$ MEFs or γ2a cells (Supplementary Fig. 3i, j) with PF resulted in reduced phosphorylation of the autophosphorylation site of PYK2 required for its activation (PYK2^{Y402}) (Supplementary Fig. 3i) accompanied by attenuated leptin induced STAT3 phosphorylation (Supplementary Fig. 3i, j) suggesting that the effect of PF is not cell line specific and is independent of JAK2. Results from these studies

Fig. 3 | FAK and PYK2 interact with and activate STAT3. HEK-293T cells were transiently transfected with 0.25 μg *Stat3* (lanes 2–10) and increasing amounts (0.25–1.75 μg) of wild-type or mutant *Fak* (FAK^{Y397F}) (**a**) or wild-type or kinase-dead (KD) *Pyk2* (**b**). The FAK^{Y397F} mutation prevents phosphorylation at Tyr^{397}, abolishing kinase activity (**a**, lanes 7–10). Total cell lysates (TCL) were immunoblotted with the indicated antibodies. The migration difference between wild-type and *Pyk2* KD reflects the GFP tag in the KD construct. **c** STAT3, PYK2, or FAK were transiently overexpressed in HEK-293T cells as indicated. PYK2 or FAK was immunoprecipitated, and TCL or the immunoprecipitated fractions were analyzed by western blot using the indicated antibodies. **d** Leptin enhances the interaction of hypothalamic focal adhesion kinases with STAT3. Lean wild-type mice received vehicle or leptin (5 mg/kg). Hypothalamic were collected 30 min later, crosslinked (10% formalin), homogenized, and immunoprecipitated with STAT3 or IgG control antibodies. Immunoprecipitates were analyzed for the indicated proteins. *Fak* and *Pyk2* mRNA (**e**) and protein (**f**) expression in N1 cells stably expressing shScr, shFak, or shPyk2 constructs. **g** LepRb-expressing N1 cells with shScr, shFak, or shPyk2 were stimulated with leptin (40 ng/mL), and pSTAT3 and total STAT3 were analyzed at the indicated times. **h** Quantification of pSTAT3/STAT3 signals; inset shows the area under the curve. **i** N1 cells transfected with *LepRb* and either shScr or shRNAs targeting both *Fak* and *Pyk2* were stimulated with 40 ng/mL leptin. Total lysates were analyzed by immunoblot for pSTAT3 and total STAT3. **j** N1 cells stably expressing LepRb and a STAT3-driven luciferase reporter were treated with PF and leptin. Luminescence was measured 24 h later. **k** Relative leptin-induced luminescence at 0, 2, and 128 ng/mL leptin with PF concentrations of 0 (Veh), 330 nM, 1 μM, or 3.3 μM. Blots are visualized with a Bio-Rad ChemiDoc Touch Imaging System. Data shown are representative of an experiment conducted once (**a**–**f**) or twice (**g**–**k**) with similar results. Data are represented as mean ± SEM and analyzed by one-way (**h**) or two-way ANOVA (**e**, **k**).

strongly suggest that FAK and PYK2 are critical regulators of leptin receptor signaling.

FAK and PYK2 mediate leptin action in vivo

Central inhibition of focal adhesion kinases attenuated the weight reducing effect of TubA in DIO mice (Fig. 2a, b), and we showed previously that TubA action is leptin dependent[44]. Hence, we decided to test if FAK and/or PYK2 regulated leptin action in vivo. To this end, we first analyzed the central expression profile of the focal adhesion kinases, which had not been previously characterized. We conducted RNAscope in situ hybridization to analyze the expression profile of *Fak* and *Pyk2* and their co-localization with *LepR* in the arcuate nucleus (ARC), ventromedial hypothalamus (VMH), and dorsomedial hypothalamus (DMH), three well-characterized sites of leptin action and TubA-induced leptin sensitivity[44]. Throughout the hypothalamus, a majority of the $LepR^+$ neurons expressed at least one of the focal adhesion kinases with more $LepR^+$ cells colocalizing with *Fak* than with *Pyk2* (Fig. 4a and Supplementary Figs. 4, 5). *Fak* has a uniform hypothalamic expression which is higher than *Pyk2* expression in the ARC, whereas *Pyk2* expression is higher in the DMH compared to the ARC and VMH (Fig. 4b and Supplementary Figs. 4 and 6a–d). We corroborated these findings by reanalyzing a publicly available hypothalamic single cell sequencing dataset[57], which corroborated that *Fak* was ubiquitously expressed and *Pyk2* expression was restricted to neurons and microglia (Supplementary Fig. 7).

To assess whether the expression of the focal adhesion kinases responds to nutritional need states or leptin, we conducted a similar study in mice subjected to fasting with or without leptin treatment, and also analyzed the published datasets for the hypothalamic expression profile of the two transcripts. We did not detect a significant effect of fasting on the expression of either gene in the ARC, VMH, or DMH, despite a tendency for increased *Pyk2* expression in the ARC (Fig. 4c–k). RNA sequencing of distinct hypothalamic nuclei ARC, VMH, DMH or PVN (paraventricular nucleus of the hypothalamus) did not display a significant regulation of *Fak* or *Pyk2* by fasting (Supplementary Fig. 7a–d). Analyzing two distinct datasets on the transcriptional profile of AgRP neurons, which are critical mediators of leptin action located exclusively in the ARC, revealed that fasting significantly increased the expression of *Fak* and *Pyk2* in the AgRP neurons but not in the POMC neurons[58,59] (Supplementary Fig. 7e–g). In agreement with this finding, our *LepR*-specific expression analysis revealed that fasting increased the expression of *Pyk2* specifically in the ARC *LepR* population (Fig. 4k).

The hypothalamic expression profiling results collectively suggested that a majority (88–94%) of $LepR^+$ neurons expressed at least one of the focal adhesion kinases. We next assessed the physiological relevance of the focal adhesion kinases in mediating leptin dependent feeding and body weight regulation in vivo. To this end, we implanted cannulas into the lateral ventricle of lean wild-type mice for direct intracerebroventricular (icv) infusion of PF. We first confirmed that icv administration of PF did not affect fasting-induced re-feeding (Fig. 5a). Intraperitoneal (ip) administration of leptin prior to the onset of the dark cycle suppressed fasting-induced food intake (Fig. 5a). Central administration of PF, however, was sufficient to suppress leptin-induced anorexia (6.09 g ± 1.14 Veh (icv)/Leptin (ip) vs. 7.22 g ± 1.58 PF (icv)/Leptin (ip) food consumed at 24 h, $p = 0.0116$) (Fig. 5a). Since the hypothalamus is a major site of leptin action, we first analyzed if PF attenuated leptin induced STAT3 phosphorylation in total hypothalamic lysates obtained from lean wild-type mice. Icv PF infusion followed by ip leptin administration impaired the leptin-induced activation of hypothalamic STAT3 (Fig. 5b, c). PF infusion did not block the leptin induced STAT3 phosphorylation completely, presumably due to the involvement of other kinases, including JAK2. Because the extent of leptin action varies across hypothalamic nuclei, we conducted a similar experiment with vehicle or PF infusion into lateral ventricle of lean mice and subsequently analyzed the kinetics of STAT3 phosphorylation in the ARC, VMH and DHM following ip PBS or leptin injections. PF-treated mice had a significantly attenuated leptin response in all three nuclei analyzed (Fig. 5c). Taken together, these results suggest that central inhibition of focal adhesion kinases inhibit leptin signaling.

We next tested the leptin response of the Pyk2 KO mice compared to their wild-type littermates. Pyk2 KO mice exhibited reduced leptin-induced food intake suppression such that they tended to eat more than the wild-type mice even in the presence of peripheral leptin administration (4.38 g ± 1.38 wild-type/Leptin, vs. 5.25 ± 1.21 Pyk2 KO/Leptin food consumed at 24 h) (Fig. 6a, b). While leptin significantly blunted the body weight gain in wild-type mice after 6 and 18 h of refeeding, this effect was not observed in the Pyk2 KO mice (Fig. 6c). Finally, leptin-induced STAT3 phosphorylation was diminished in the KO cohort (Fig. 6d, e), in line with our previous findings. Altogether, these results suggest that focal adhesion kinases are required for the full anorectic effect of leptin.

To directly determine the role of hypothalamic focal adhesion kinases in the regulation of energy metabolism, we first designed AAV particles encoding a scrambled shRNA sequence or two tandem shRNA sequences targeting *Pyk2* and *Fak* (shPyk2/Fak). We aimed for dual knockdown due to the redundant function of the two kinases and to avoid potential compensatory expression in response to a single focal adhesion kinase gene knock down[22–25] (Fig. 3e). We injected these AAV particles into the mediobasal hypothalamus (covering ARC and VMH) and DMH of adult lean mice (Supplementary Fig. 8a). Two weeks after viral injection, we placed half of the mice in either AAV group (shScr versus shPyk2/Fak) on HFD. Mice in the shPyk2/Fak groups developed obesity on both regular chow and HFD (Fig. 7a–c). On either diet, shPyk2/Fak cohorts consumed more food (Fig. 7d), accounting for their rapid weight gains, which was reflected in significant accumulation of fat mass (Fig. 7e–h) and elevated fasting blood glucose (Fig. 7i).

https://doi.org/10.1038/s41467-026-69008-9

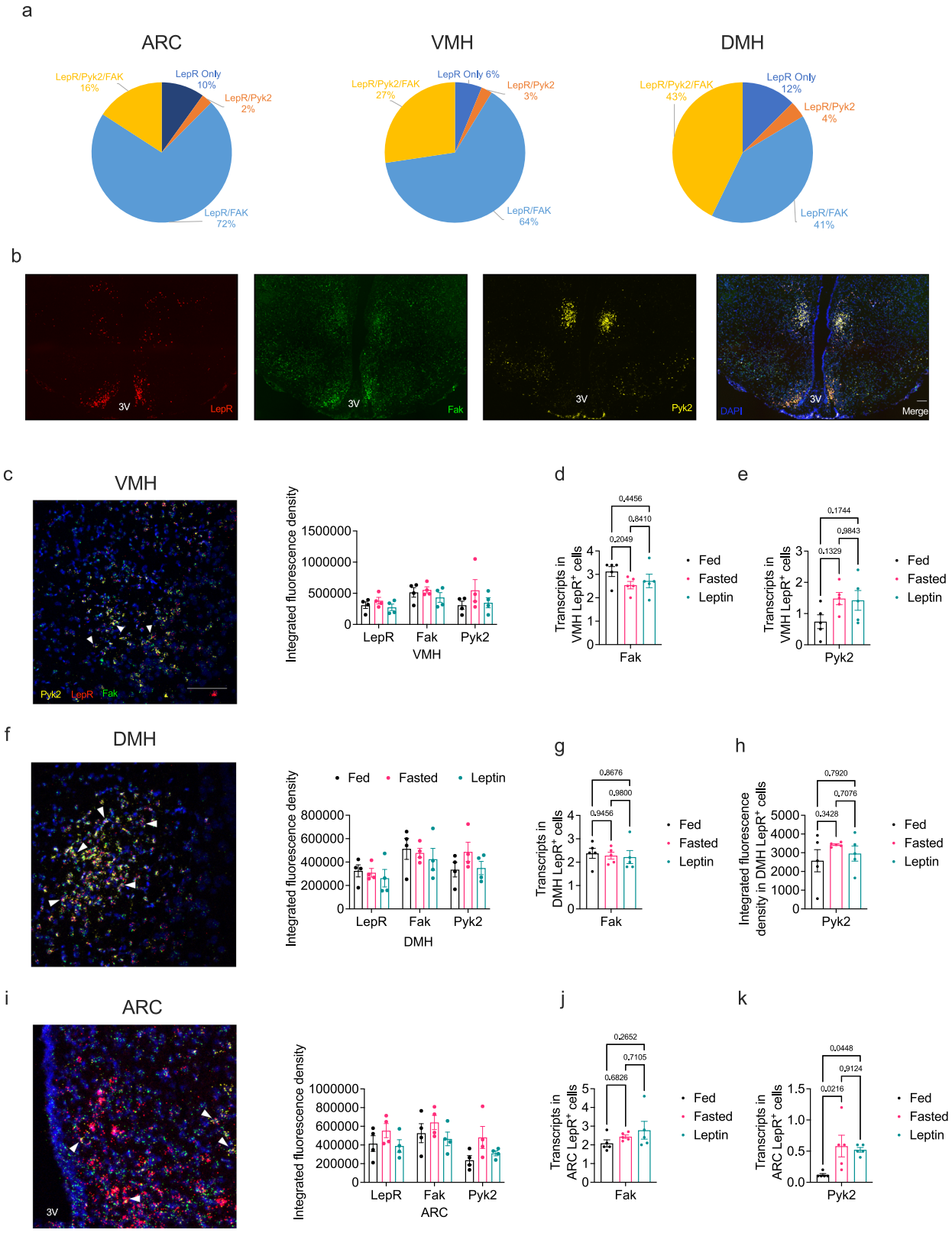

Before the development of any significant weight difference, we also tested the leptin response of the mice on chow diet. While leptin suppressed the food intake and weight gain of the shScr group, dual knockdown of the kinases in the hypothalamus (shPyk2/Fak group) impaired the anorectic action of leptin (Fig. 7j, k), confirming our previous findings that focal adhesion kinases are indispensable for leptin action in vivo. Taken together, these findings strongly suggest that hypothalamic action of focal adhesion kinases is required for leptin receptor signaling and the maintenance of energy homeostasis.

HDAC6 inhibitors induce weight loss in a leptin dependent manner[44,45,60]. Therefore, we finally tested the weight reducing effect of HDAC6 inhibitors on DIO shPyk2/Fak cohort and their control group. Following an acclimation period, where mice maintained stable body weights, we treated the DIO cohorts with TubA. Animals in the shScr

Fig. 4 | Hypothalamic expression profile of the focal adhesion kinases. **a**–**k** Hypothalamic sections from lean wild-type mice, ad libitum fed, overnight fasted, or overnight fasted and leptin (3 h) treated (ip) were stained with fluorescent RNAscope probes targeting *LepR*, *Fak* or *Pyk2* transcripts. **a** The percent of *LepR*⁺ cells with *Fak* and *Pyk2* in the ARC, VMH, and DMH. **b** Representative images of hypothalamic sections covering ARC, VMH, and DMH for *LepR*, *Fak*, *Pyk2* expressions. The scale bar represents 100 µm. Representative RNAscope images and region specific and *LepR*⁺ specific transcript quantification in the VMH (**c**–**e**), DMH (**f**–**h**), and ARC (**i**–**k**) ($n = 5$ mice per group). Red: *LepR*, yellow: *Pyk2*, green: *Fak*, blue: DAPI. Arrowheads indicate triple colocalization of *LepR*, *Pyk2*, and *Fak*. The scale bar represents 50 µm (**c**). The transcripts in the *LepR*⁺ cells were expressed as the counted pixels within the *LepR*⁺ cells, except for *Pyk2* signal in the DMH, which is expressed as the total fluorescence due to high signal intensity. Data shown are representative of an experiment conducted once. Data are represented as mean ± SEM and are analyzed by one-way ANOVA (**d**, **e**, **g**, **h**, **j**, **k**).

group displayed decreased food intake and weight loss following TubA administration (Fig. 7l–n). However, dual knockdown of the kinases led to resistance to the anti-obesity effect of TubA (Fig. 7l–n). Loss of response to TubA was not due to excess obesity of the sh*Pyk2*/*Fak* cohort as we observed a similar effect in a sub-cohort of mice selected for matched pre-treatment body weights (Fig. 7o). Notably, these results were not restricted to TubA. Mice in the DIO shPyk2/Fak group maintained their body weight during treatment with the brain penetrant HDAC6 inhibitor ACY775, which induced weight loss in DIO shScr mice (Supplementary Fig. 8b–f), collectively suggesting that central action of focal adhesion kinases is required for the anti-obesity effect of HDAC6 inhibitors.

Discussion

In this work, we utilized the gene expression signatures representing activated leptin receptor signaling and identified the focal adhesion kinases as central regulators of energy metabolism and leptin sensitization. Our previous findings indicated that HDAC6 inhibitors induce central leptin sensitization primarily through their peripheral action (Fig. 7 and discussed in more detail below). While DIO mice display central leptin resistance, the hypothalamic gene expression profile of TubA-treated DIO mice reflects a leptin sensitized state. We combined this TubA-induced DIO gene expression signature with the hypothalamic profile obtained from leptin-treated lean mice. These gene expression signatures representing leptin re-sensitized and leptin-induced states negatively correlated with the transcriptomics profile induced by focal adhesion kinase inhibition, thereby motivating us to study the role of FAK and PYK2 in leptin receptor signaling and HDAC6-inhibition-induced weight loss.

Leptin stimulates multiple downstream signaling pathways, however leptin-induced activation of STAT3 is the predominant branch leading to the homeostatic control of feeding and body weight[7]. While JAK2 is the canonical STAT3 kinase in response to leptin stimulation, existence of in vitro JAK2-independent but STAT3-dependent leptin signaling mechanisms[10] further prompted our investigation into the involvement of the focal adhesion kinase family in leptin signaling. We identified that FAK and PYK2 act as STAT3 kinases downstream of LepRb, their interaction with STAT3 was promoted upon leptin stimulation, and their activity is required for the full activation of STAT3 by leptin and the weight reducing effect of HDAC6 inhibitors. In this regard, it is worth investigating whether focal adhesion kinases are utilized by other leptin sensitization or weight loss pathways.

While most *LepR*⁺ neurons in the ARC, VMH and DMH are positive for *Fak* (84–91%), *Pyk2* has a more restricted expression profile, representing between 30–50% of *LepR*⁺ cells in the hypothalamus. The functional redundancy between the two kinases[25,61] and the relatively lower expression of *Pyk2* potentially explains why the DIO Pyk2 KO mice have compromised but not completely blunted response to TubA-induced weight loss and normal body weight gain on HFD. When the two kinases are pharmacologically inhibited in the brain or genetically targeted in the hypothalamus, we observed a more potent attenuation of leptin action in lean mice and the TubA/ACY775 action in DIO mice. An outstanding question remains regarding how peripheral HDAC6 inhibition is linked to the central action of the focal adhesion kinases. Following TubA administration, the hypothalamic expression of *Fak* and *Pyk2* increases, suggesting a potential transcriptional regulation. Furthermore, this regulation appeared to be leptin dependent as TubA failed to increase the hypothalamic expression of either kinase in *db/db* mice (*Fak*: 1.00 ± 0.045 Veh vs. 1.00 ± 0.027 TubA, $p = 0.92$; *Pyk2*: 1.00 ± 0.049 Veh vs. 1.16 ± 0.117 TubA, $p = 0.26$ by *t*-test), which helps explain why HDAC6 inhibition does not exert weight loss in *db/db* mice. It is possible that the peripherally derived factor(s) that mediate the leptin sensitizing effect of HDAC6 inhibition (graphical abstract) is responsible for such a transcriptional regulation. Among the hypothalamic nuclei and neuronal populations, we investigated, *Pyk2* and *Fak* expression in the ARC and AgRP neurons, which mediate majority of leptin action, were most sensitive to nutritional state. Fasting selectively increases the expression of focal adhesion kinases and leptin receptor in this orexigenic cell population as opposed to the anorexigenic POMC neurons. Whether such a response to fasting is important for the acute regulation of feeding or energy expenditure—beyond fasting induced leptin sensitivity—is unknown.

The findings presented here on the role of focal adhesion kinases in energy metabolism could likely extend beyond the regulation of leptin signaling. The role of FAK and PYK2 in the regulation of STAT3 downstream of secreted factors other than leptin in a myriad of biological processes is worth investigating. Furthermore, focal adhesion kinases are involved in several cellular processes developmentally critical for energy homeostasis including neuronal growth and synaptic plasticity[62]. Since leptin also acts a neurotrophic factor[63], the focal adhesion kinases could conceivably play a critical role in the leptin-induced neuronal remodeling and related central functions beyond energy metabolism such as learning and memory. Likewise, leptin action is critical for the regulation of glucose homeostasis and fertility. While our study demonstrated the role of the focal adhesion kinases in the regulation of energy balance, the potential contribution of the focal adhesion kinases to other leptin-regulated physiological parameters are worth investigating.

During the revision of our manuscript, another group also showed that HDAC6 inhibitors reduce obesity by improving central leptin sensitivity but proposed a cell-autonomous mechanism of leptin sensitization[64]. The authors suggested that leptin receptor is a substrate of HDAC6 and that acetylation of leptin receptor increased leptin-induced STAT3 phosphorylation. We repeated some of the key experiments proposed by this group. In direct contrast to the authors' findings, we did not detect an effect of HDAC6 overexpression in leptin-induced STAT3 phosphorylation. In accordance with our previous findings[44], none of the three different HDAC6 inhibitors we tested increased leptin receptor signaling in a controlled in vitro system (Supplementary Fig. 9), suggesting that HDAC6 does not regulate leptin receptor signaling cell autonomously. Notably, in recapitulating the authors' system, we noticed that the acetyltransferase p300 augmented the leptin receptor signaling due to an artifact of the overexpression system such that p300 overexpression led to increased expression of LepRb from the co-transfected plasmid (Supplementary Fig. 10). This effect was not restricted to LepRb as p300 overexpression also increased *GFP* and *LacZ* gene expressions (Supplementary Fig. 10), suggesting that the effect of p300 overexpression on

https://doi.org/10.1038/s41467-026-69008-9

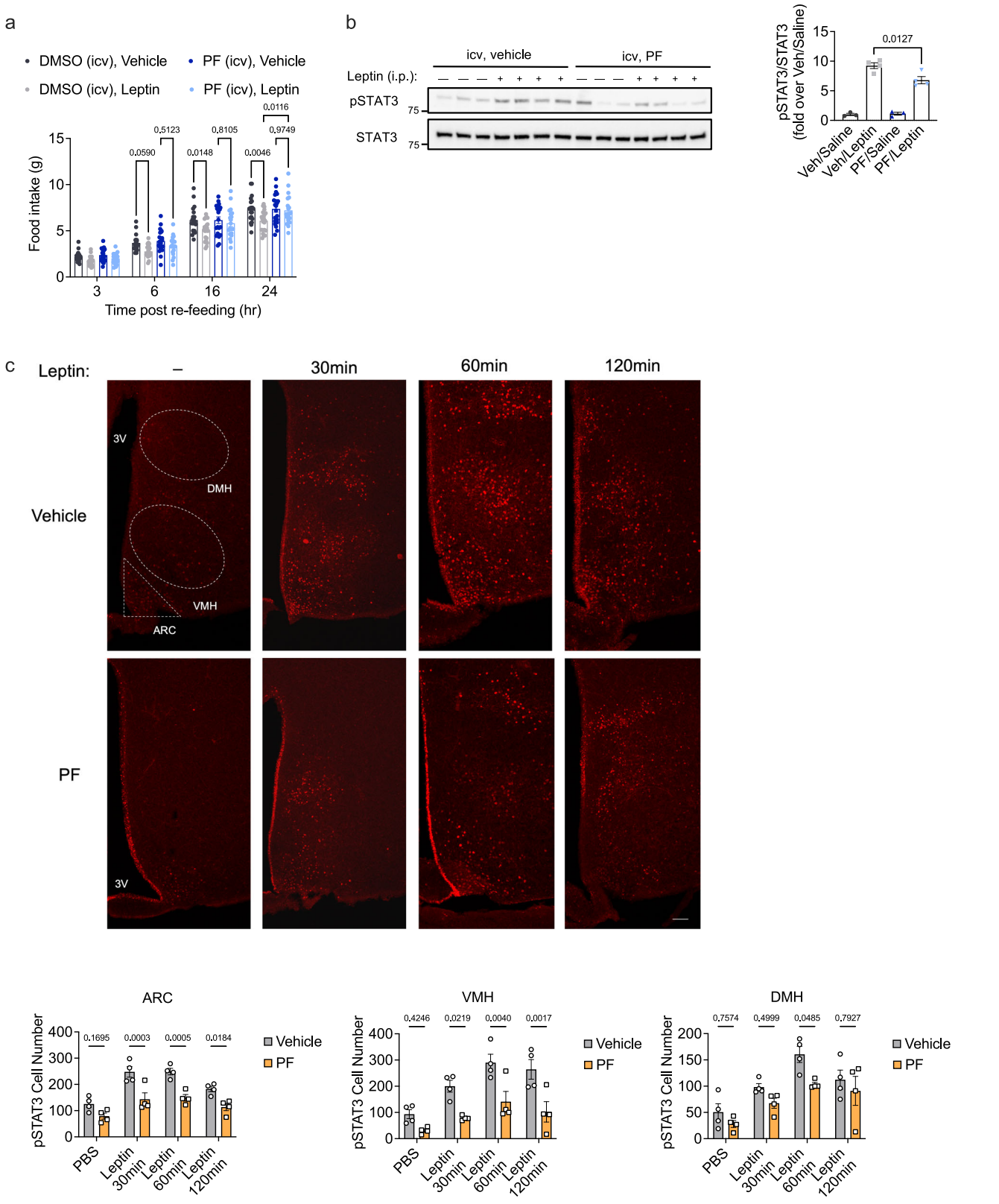

seemingly elevated leptin signaling is an artifact of this in vitro system and is independent of the promoter the transgenes were expressed from (Supplementary Fig. 10). We observed that the p300-related acetyltransferase CBP (CREB Binding Lysine Acetyltransferase) also had a similar effect on the expression of genes that are co-transfected with it (Supplementary Fig. 10), suggesting that this effect might be common for acetyltransferases. In agreement with the cell nonautonomous effect of HDAC6 inhibition on leptin sensitization and weight loss, we previously showed that central infusion of HDAC6 inhibitors to DIO mice strongly inhibited central HDAC6 activity but did not reduce body weight. These results combined with the observations that neuronal[44] or AgRP-specific[64] HDAC6 deletion does not prevent obesity whereas adipose specific HDAC6 KOs are resistant to weight gain and hyperglycemia[44], and that TubA-treated mice secrete a

https://doi.org/10.1038/s41467-026-69008-9

Fig. 5 | Focal adhesion kinases regulate leptin action in vivo. a Fasted lean wild-type mice implanted with a cannula into the lateral ventricle were administered DMSO (Vehicle) or PF (2.5 μg) by intracerebroventricular (icv) route. One hour later, mice were administered either saline or leptin ip and food was provided. Food intake was measured at 3, 6, 16, and 2 h ($n = 20$ DMSO + Vehicle mice; $n = 21$ DMSO + Leptin mice; $n = 21$ PF + Vehicle mice; $n = 20$ PF + Leptin mice). **b** Lean wild-type mice fasted overnight were administered vehicle or PF icv 15 min later, mice received an ip injection of either saline or leptin. 30 min later, hypothalamic punches were collected and snap frozen in liquid nitrogen for analysis by immunoblot. Blots are visualized with a Bio-Rad ChemiDoc Touch Imaging System. Quantification of the western blot is shown on the right ($n = 3$ mice per group). **c** pSTAT3^{Y705} IHC staining of the hypothalamic sections of lean wild-type mice. Animals were centrally infused with vehicle or PF, and treated with saline or leptin 15 min later. Brains were removed and prepared for IHC staining 30, 60 or 120 min after leptin injections. pSTAT3 positive cell number across the ARC, VMH, and DMH are quantified. The scale bar represents 100 μm. Data shown are representative of an experiment conducted once (**c**), twice (**b**) or three times (**a**) in separate cohorts of animals with similar results. Data are represented as mean ± SEM and analyzed by one-way (**b**) or two-way ANOVA (**a**, **c**).

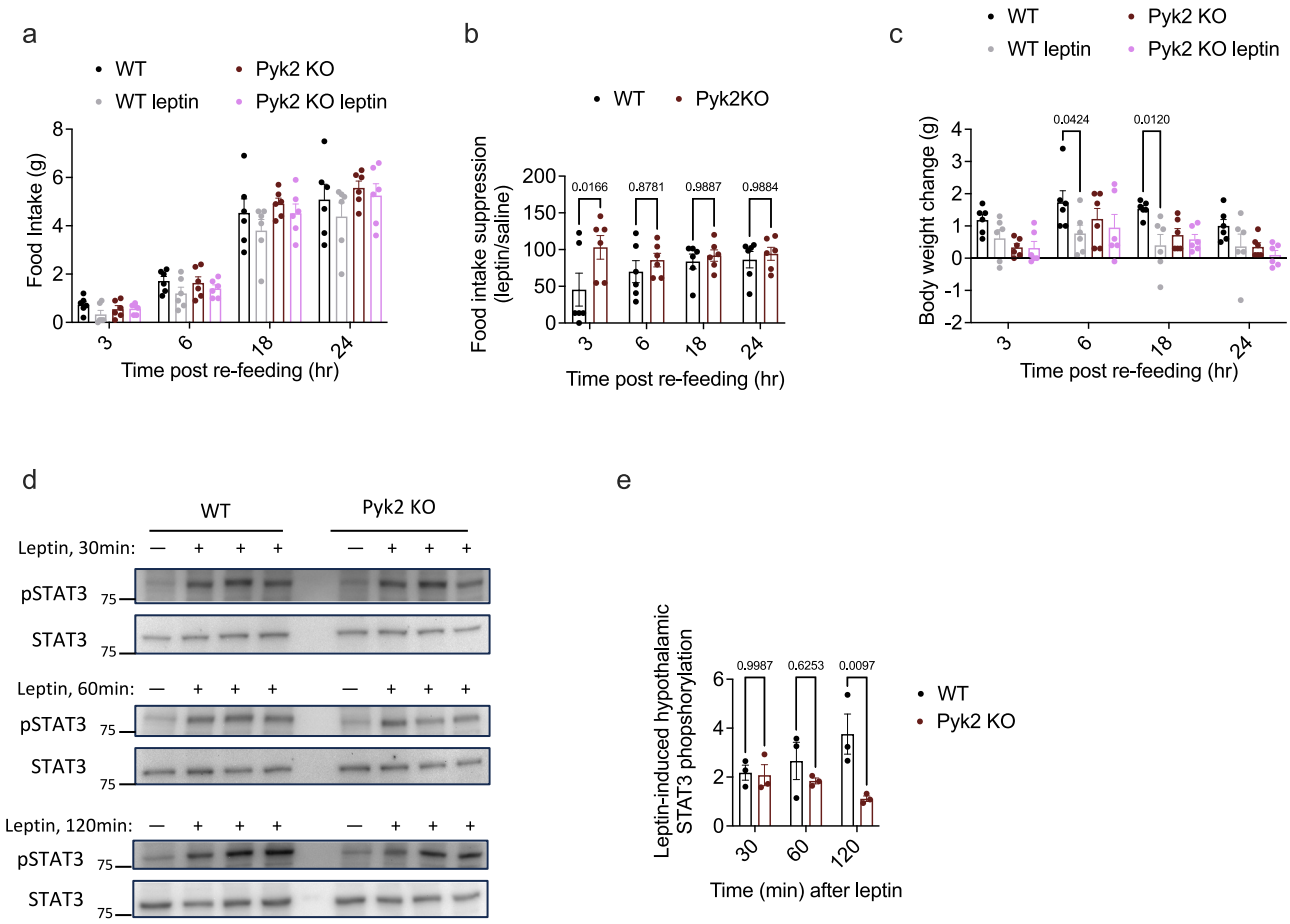

Fig. 6 | Pyk2 KO mice have impaired leptin sensitivity. a–**c** Fasted lean wild-type and Pyk2 KO mice were treated (ip) with vehicle or leptin, and food intake and body weights were followed for 24 h. **a** Time course of food intake, **b** food intake presented as normalized to the respective vehicle groups, and **c** weight change of the animals (**a**–**c**, $n = 6$ mice per group). **d**, **e** Hypothalamic STAT3 phosphorylation was analyzed 30, 60, and 120 min post leptin injection in lean wild-type and Pyk2 KO mice ($n = 1$ Vehicle mouse; $n = 3$ Leptin mice, per timepoint). Blots are visualized with a Bio-Rad ChemiDoc Touch Imaging System. Data shown are representative of experiments conducted twice in separate cohorts of animals with similar results. Data are represented as mean ± SEM and are analyzed by two-way ANOVA.

protein-based factor that can directly induce leptin sensitization, strongly supports our two-site-of-action model where peripheral HDAC6 inhibition is coupled to central leptin sensitization though a yet unidentified factor (Fig. 8).

Our study has utilized male mice for all the experiments and is therefore has the limitation of not directly addressing the role of sex as a biological factor. *Fak* or *Pyk2* do not display a significant expression difference in male versus female human hypothalamus samples in the Genotype-Tissue Expression (GTEx) Portal ($p = 0.091$ and 0.59, for *Pyk2* and *Fak*, respectively by Wilcoxon test), and we previously showed that HDAC6 inhibition induces weight loss also in female DIO mice[44], suggesting that the role for focal adhesion kinases in leptin signaling is independent of sex. However, future research will reveal the potential expression difference and role of *Fak* or *Pyk2* in *LepR* positive neurons of male and female animals.

Leptin action is mediated by multiple sites in the central nervous system with the leptin receptor expressing neurons in the hypothalamic arcuate nucleus and the DMH playing the predominant role[65]. In our study we targeted the focal adhesion kinases in these two regions to demonstrate their indispensable role in leptin action. Future studies will demonstrate the contribution of each enzyme in genetically defined leptin receptor positive cell populations, including the AgRP, POMC and the recently identified GABAergic BNC2 positive cells[66–68], to the anorectic effect of leptin. In this regard, it is important to note that the several factors including neuronal plasticity, redundancy between the proteins at the cell autonomous level

https://doi.org/10.1038/s41467-026-69008-9

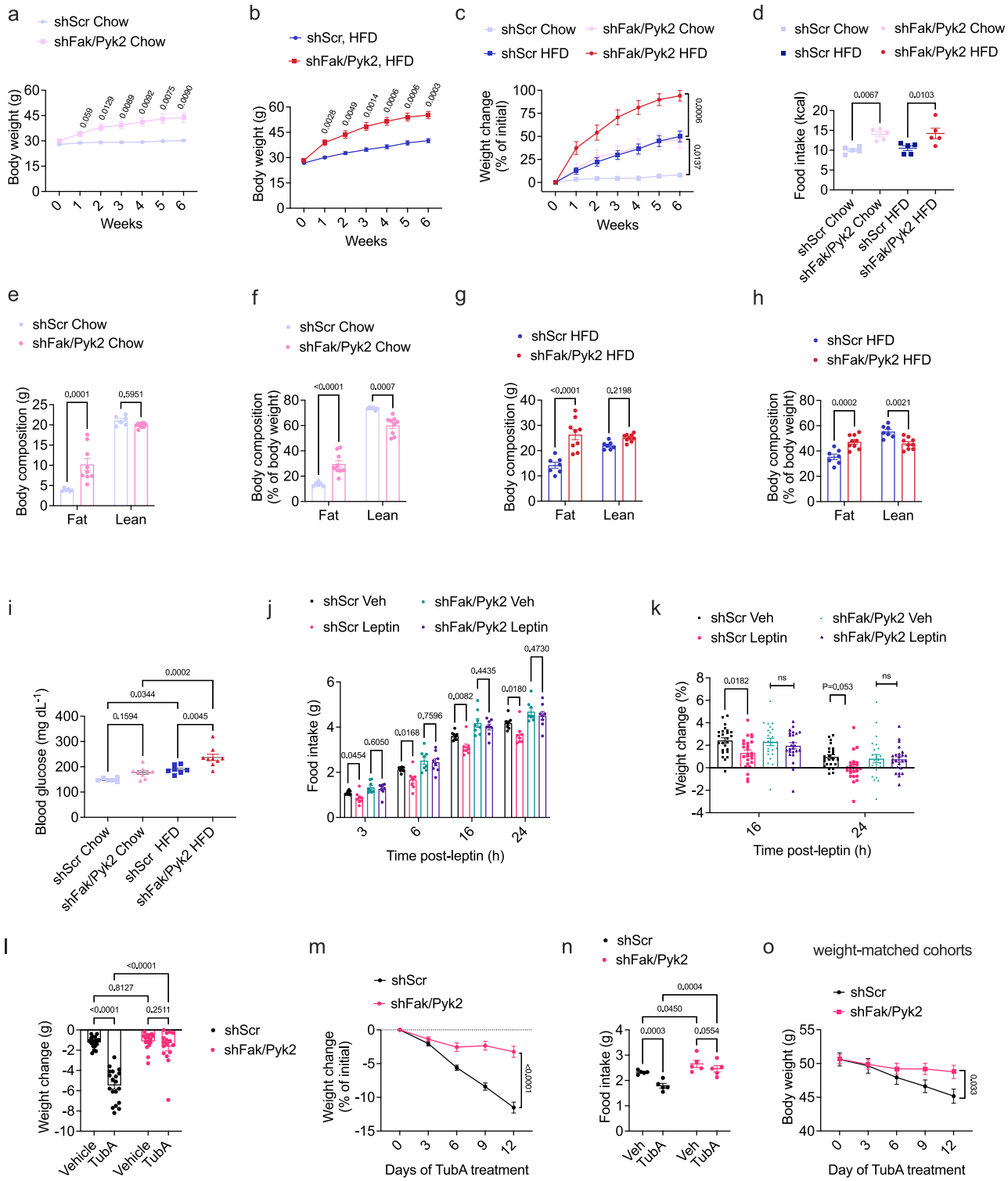

Fig. 7 | Hypothalamic focal adhesion kinases regulate energy metabolism. Lean wild type mice were bilaterally injected with AAV particles encoding shScr or shPyk2/Fak in the mediobasal hypothalamus and DMH. Two weeks later mice were either maintained on regular chow or switched to HFD. **a**–**c** Growth curves of the cohorts on the indicated diets expressed either as absolute body weight or percent weight gain. Week 0 indicates 2 weeks post viral injection. **d** Food intake of the cohorts measured over 24 h around week 3. Body composition of the cohort measured around week 2 using NMR and plotted as absolute tissue mass (**e**, **g**) or normalized to body weight (**f**, **h**). **i** Blood glucose of the mice measured during the daytime after a 4 h fast (**a**–**i**, $n = 6$ shScr Chow mice; $n = 7$ shScr HFD mice; $n = 9$ shFak/Pyk2 mice). Cohorts on chow diet (group caged) were treated with either vehicle or leptin (5 mg/kg, ip) prior to dark cycle and their food intake (**j**) ($n = 8$ mice per group) and body weight (**k**) was followed for 24 h ($n = 25$ shScr mice; $n = 24$ shFak/Pyk2 mice). **l**–**o** DIO cohorts were treated with vehicle or TubA (15 mg/kg, ip, daily). Absolute weight change (**l**), percent weight change (**m**), average food intake (**n**), and body weights (**o**) are measured daily (**l**–**o**, $n = 19$ shScr mice; $n = 16$ shFak/Pyk2 mice). Data shown are representative of experiments conducted twice in separate cohorts of animals with similar results. Data are represented as mean ± SEM and are analyzed by one-way (**d**, **i**) or two-way ANOVA (**a**–**c**, **e**–**h**, **j**–**o**).

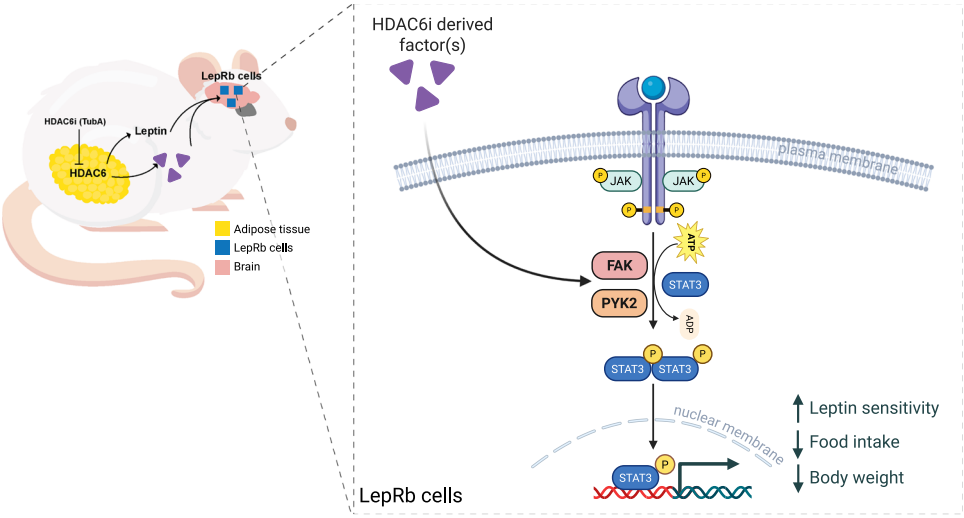

Fig. 8 | HDAC6 inhibition regulates central leptin signaling through focal adhesion kinases. Peripheral HDAC6 inhibition induces a systemic signal(s) of unknown nature (depicted as purple triangle) that act as leptin sensitizers leading to weight loss in diet-induced obese mice. Central inhibition or genetic ablation of HDAC6 does not induce weight loss. This cell non-autonomous mechanism involves increased expression of the focal adhesion kinases, FAK and PYK2, which can directly phosphorylate the transcription factor STAT3 acting downstream of leptin receptor. STAT3 is also phosphorylated by its canonical kinase, JAK2, in response to leptin. Phosphorylated STAT3 translocates to the nucleus and induces a transcriptional program leading to suppression of food intake and increased energy expenditure. Created in BioRender. Cakir, I. (2026) https://BioRender.com/jd9puvs.

and their effect at acute versus chronic level should be accounted for while evaluating the relative importance of factors acting downstream of the leptin receptor. For example, phosphoinositide 3-kinase (PI3K) signaling regulates acute but not chronic responses to leptin action[69]. In our studies, Pyk2 KO mice displayed normal body weights also on HFD compared to the wild type littermates, in contrast to a previous report on Pyk2 KO mice being more obesity prone[42]. While the reason for this discrepancy is not clear, we propose that the embryonic ablation of *Pyk2* is compensated by FAK or other kinases, including JAK2 and Src[10,70–73], leading to a normal phenotype. The predominantly DMH-localized expression of *Pyk2* is also in agreement with the phenotype we report here for the global Pyk2 KO mice. Considering the redundancy between the two kinases for various cellular activities, the difference in their hypothalamic expression profile, and the fact that both genes are also expressed outside the central nervous system, we targeted both kinases in the DMH and the mediobasal hypothalamus to specifically study their central action. Our results collectively document the indispensable role of focal adhesion kinases in the regulation of feeding primarily through leptin receptor signaling and provide key evidence for the focal adhesion kinases acting as key mediators of leptin resensitization secondary to peripheral HDAC6 inhibition (Fig. 8).

We have previously shown that peripheral HDAC6 inhibition, primarily through the adipose tissue sends a systemic signal to the brain to confer leptin sensitization[44]. Hence, an inter-tissue signaling molecule integrates the function of HDAC6 and focal adhesion kinases acting at distant tissues to the regulation of energy metabolism at the level of leptin receptor signaling.

Methods

Mice

All animal studies were performed following procedures approved by the Institutional Animal Care and Use Committees (IACUC) at the University of Michigan and University of Pittsburgh, and by the Committees on Ethics of Animal Experiments of the University of Pavia. Mice were fed either regular chow (5LOD from Lab Diet, Purina, St. Louis, MO) or high-fat diet (HFD, 60 kcal% fat, Research Diets, cat. no. D12492) and had free access to food and water unless noted otherwise and kept on a 12 h light/dark cycle in a temperature and humidity-controlled environment. Mice had ad libitum access to food and water unless otherwise indicated. Wild-type male C57BL/6J mice (The Jackson Laboratory, Bar Harbor, ME) were used. Pyk2 KO mice generation was previously reported[19] and colonies were maintained as described[26]. Only male mice were included in this study.

Cannulation surgery

Mice were anesthetized with isoflurane, and a stainless-steel guide cannula (Plastics One, Roanoke, VA) was implanted into the lateral ventricle using the following stereotaxic coordinates: AP: −0.46 mm, ML: −1.00 mm, DV: −2.20 mm. All intracerebroventricular (icv) injections were performed using a 2-μL Hamilton syringe (Plastics One, Roanoke, VA). Following recovery from the surgery, accurate placement of the cannula was confirmed by central angiotensin II administration. Animals that did not exhibit an elevation in water intake in response to central angiotensin II were excluded from the study. PF was dissolved in DMSO and infused at 500 nL per mouse into the right lateral ventricle at the indicated doses.

Stereotaxic viral injections

Mouse *Pyk2*- and *Fak*-targeting shRNA sequences described above were cloned into an AAV vector in tandem reading frames (VectorBuilder). AAV2-CMV-*Pyk2*/*Fak* shRNA and AAV2-CMV-scramble shRNA viruses were generated by the University of Michigan Vector Core. For stereotaxic surgical procedures, 8 to 10-week-old wild-type mice were anesthetized with isoflurane and positioned in a stereotaxic frame (Kopf). A micro-precision drill was used to create a small burr hole directly above the site of viral injection, followed by the careful removal of the dura. A total of 500 nL of AAV was injected bilaterally into the arcuate nucleus and dorsomedial hypothalamus using a micromanipulator (Narishige) attached to a pulled glass pipette. The coordinates from bregma for the arcuate nucleus: anterior/posterior: −1.40 mm, medial/lateral: ±0.25 mm, dorsal/ventral: 5.95 mm; for DMH: anterior/posterior: −1.70 mm, lateral: ±0.30 mm, dorsal/ventral: −5.60 mm. The virus was administered at a rate of 50 nL/min. After the injection, the glass pipette was left in place for an additional 10 min to prevent the viral solution from leaking outside the targeted brain

region. A recovery period of 3 weeks was allowed post-surgery to ensure viral expression and healing from the surgical procedures. Viral expression was verified post hoc in all animals. Data from animals in which the viral expression was located outside the targeted area were excluded from analysis.

Fasting and re-feeding studies

For experiments involving wild-type lean mice, food was removed from the cages of cannulated mice prior to the beginning of the dark cycle (6:00 p.m.). After 23 h of fasting, mice were infused with PF (2.5 μg as indicated in Fig. 5 legend) or DMSO vehicle of equal volume (500 nL per mouse) icv 30 min later, mice were injected with 5 or 10 mg/kg leptin or PBS as vehicle intraperitoneally (ip). Food intake was monitored 3, 6, 16, and 24 h. Body weight was measured 6, 16, and 24 h post re-feeding. This experiment was conducted on two separate cohorts of mice with both cohorts exhibiting similar results. For each cohort of mice, the fasting-induced re-feeding experiment was performed 2–3 times, each time rotating the mice in the experimental groups. Each trial was separated by a minimum of 5 days. Following the final trial, mice were fasted overnight for 16 h (6:00 p.m. to 10:00 a.m.). After the fast, PF or DMSO was injected icv, followed by leptin or PBS ip injection 15 min later. Thirty minutes after administration of leptin or PBS, hypothalamic tissue punches were collected and snap frozen in liquid nitrogen, and stored at −80 °C until further analysis. To test the effect of PF on TubA-induced weight loss (Fig. 2a, b), wild-type DIO mice on HFD were cannulated in the lateral ventricle, and treated with PF or DMSO icv and TubA or Vehicle ip once daily. For experiments involving Pyk2 KO mice, food was removed from the cages for the last 6 h prior to the onset of dark cycle. Fifteen minutes prior to the onset of the dark cycle, Pyk2 KO or littermate control mice were injected with PBS or leptin (5 mg/kg) followed by returning food to the mice. Body weight and food intake were measured 3, 6, 18, and 24 h following re-administration of food.

Antibodies and plasmids

Anti-phosphoSTAT3^{Y705} (#9145 and #9131, 1:1000), anti-STAT3 (#9139, 1:1000), anti-phosphoPYK2^{Y402} (#3291, 1:1000), anti-PYK2 (#3480, 1:1000), anti- GAPDH HRP conjugate (#8884, 1:10,000), anti-phosphoFAK^{Y397} (#8556, 1:1000), and anti-FAK (#13009, 1:1000), anti-alpha Tubulin (#3873, 1:5000), anti-acetyl alpha tubulin (#5335, 1:2000), anti-FLAG tag (#14793, 1:5000), anti-myc tag (#2278, 1:2000) HRP-conjugated anti-rabbit IgG (#7074, 1:2000), HRP-conjugated anti-mouse IgG (#7076, 1:2000), DyLight 800-conjugated anti-rabbit IgG (#5151, 1:10,000), DyLight 680-conjugated anti-mouse IgG (#5470, 1:10,000) antibodies were purchased from Cell Signaling Technology Inc. (Danvers, MA) and were diluted as indicated. The anti-α-FLAG (#SAB4301135, 1:10,000) antibody was purchased from Sigma-Aldrich (St. Louis, MO).

The FLAG-tagged human leptin receptor ORF was purchased from Sino Biologicals (Beijing, China). The wild-type human *Pyk2* ORF was purchased from OriGene (Rockville, MD). The GFP-tagged kinase-dead PYK2 mutant (PYK2 KD) was kindly provided by Dr. Kristiina Vuori (Sanford Burnham Prebys Medical Discovery Institute, La Jolla, CA). The wild-type *Fak* (#50515), autophosphorylation-site mutant FAK^{Y397F} (#50516), FLAG-tagged *Stat3*, and *LacZ* constructs were obtained from Addgene (Cambridge, MA).

In silico connectivity map (CMap) analysis

Bulk RNA sequencing was conducted using hypothalamic RNA obtained from male wild-type DIO mice treated with vehicle (dimethyl sulfoxide, DMSO) or TubA for four consecutive days. The leptin-induced gene expression changes in LepR neurons was previously published[46], and in our analysis we used the results obtained 10 h after leptin treatment. Upregulated (fold change ≥1.50) and downregulated (fold change ≤0.70) transcripts were entered into the 1.0 query version of CMap (clue.io). TubA and leptin gene expression signatures were analyzed as individual queries. The arithmetic mean of CMap derived connectivity scores for these two queries is used as the TubA/Leptin combined score. The top four perturbagens that best correlated with the combined scores were Serpin1d knockdown and kinetin-riboside (apoptosis/mitophagy inducer) as positively associated factors (changing the gene expression in the same direction as input), and ZG-10 (JNK inhibitor) and PF-562271 (PF, focal adhesion kinase inhibitor) as negatively associated factors, i.e., changing the gene expression in the opposite direction compared to the input query (Fig. 1e, f). This final list was manually sorted and some of the factors were eliminated as non-likely candidates. For example, Serpind1 is a serine protease inhibitor that is a predominantly liver-specific gene with a restricted expression to the vascular leptomeningeal cells in the brain (http://mousebrain.org/). We further ruled out Serpind1 because its over-expression had a very low similarity score (−3.125) in contrast to the relatively high score of its knockdown (85.08, with CMap similarity scores ranging between −100 to +100). Some factors in either list appeared as both negative and positive correlators, e.g., JNK inhibitors and topoisomerase inhibitors appeared with combined connectivity scores ranging from −97.49 to +35.63. We reasoned those factors were random associations due to lack of a uniform direction in their scores.

Generation of N1Stat3Luc stable cell line and experimentation

Lentivirus encoding a luciferase reporter construct under a minimal CMV promoter and a STAT3 transcriptional response element was purchased from Cellomics Technology (Halethorpe, MD). For generating the N1Stat3Luc cell line, 10 μg/mL polybrene (Santa Cruz Biotechnology, Dallas, TX) was added to the viral particles prior to addition of lentiviral medium to N1 cells. Cells were supplemented with equal volume of 10% fetal bovine serum (FBS) in Dulbecco's modified Eagle's medium (DMEM, Invitrogen, Carlsbad, CA) approximately 4 h after lentiviral medium addition. Two days after infection, the medium was removed and replaced with DMEM supplemented with 10% FBS and 10 μg/mL puromycin antibiotic selection (Thermo Fisher Scientific, Waltham, MA). Surviving cells which had stably integrated the construct (denoted as N1Stat3Luc) were used for experiments. For experiments using the N1Stat3Luc cells, cells were plated in 384 well plates. On the following day, cells were transfected with 80 ng *LepRb* and 0.12 μL Lipofectamine 2000 (Invitrogen, Carlsbad, CA) in reduced serum medium (Opti-MEM, Invitrogen, Carlsbad, CA). The following day, the indicated concentration of PF and leptin was added. The following day, 1x D-luciferin substrate was added to each well. Within 10 min of D-luciferin addition, fluorescence was measured using an EnSpier plate reader (PerkinElmer, Waltham, MA).

Cell culture and transfection

All cell lines were maintained at 37 °C in 5% CO_2 in DMEM supplemented with 10% heat-inactivated FBS and 100 units/mL penicillin, 100 μg/mL streptomycin or selection antibiotic. The embryonic mouse hypothalamus cell line (N1) was purchased from Cedarlane Labs (Burlington, Canada). The JAK2$^{-/-}$ mouse embryonic fibroblasts and γ2a human fibroblasts, which were both kindly provided by Dr. Liangyou Rui (University of Michigan, Ann Arbor, MI), stably express LepRb as previously described[10] and were maintained in 100 μg/mL hygromycin B (Invitrogen, Carlsbad, CA) selection. Upon transfection, medium containing antibiotics was removed and replaced with DMEM with 10% FBS. Plasmids were transfected using Lipofectamine 2000 (Invitrogen, Carlsbad, CA) in accordance with the manufacturer's protocol.

Generation of *Fak* and *Pyk2* stable knockdown cell lines

Fak (CCGGGCCTTAACAATGCGTCAGTTTCTCGAGAAACTGACGCATTGTTAAGGCTTTTTG) and *Pyk2* (CCGGATTGAGGACGAAGACTATTACCTCGAGGTAATAGTCTTCGTCCTCAATTTTTTG) shRNA constructs

were purchased from Sigma (St. Louis, MO). Scramble shRNA (plasmid #1864) was purchased from Addgene. Scramble shRNA construct in pLKO.1 vectors was subcloned into pLL3.7 (#11795, Addgene), which also encodes GFP. Lentivirus was generated by transfecting 293 T cells plated in 15 cm dishes with the following plasmids: 6.3 μg each of pRSV-Rev, pVSVG, and pMDLp/g (gift of Dr. Roger Colbran, Vanderbilt University) and 12.6 μg of the shRNA construct. Ninety-six hours following transfection, the medium was collected, briefly centrifuged, and filtered through a 0.45 μm filter. Lentiviral medium with 10 μg/mL polybrene (Santa Cruz Biotechnology, Dallas, TX) was added to N1 cells which were supplemented with equal volume of 10% FBS DMEM approximately 4 h after lentiviral medium addition. Two days after infection, the medium was removed and replaced with DMEM supplemented with 10% FBS and 10 μg/mL puromycin antibiotic selection (Thermo Fisher Scientific, Waltham, MA). Surviving cells which had stably integrated the construct were used for experiments as indicated.

RT-qPCR

Total RNA was extracted using TRIzol (Invitrogen, Carlsbad, CA). Isolated RNA was converted to cDNA using a cDNA Reverse Transcription Kit (Invitrogen, Carlsbad, CA). Using the generated cDNA, gene expression was analyzed by qPCR using forward and reverse primers (listed below) for the indicated genes and SYBR Green qPCR Master Mix (Invitrogen, Carlsbad, CA). All primers used for qPCR were purchased from Sigma-Aldrich (St. Louis, MO). An ABI Prism 7500 FAST sequence detector (Applied Biosystems) was used to run the qPCR reaction. The ΔΔCT method was used to determine the expression level of a given transcript which was normalized to a housekeeping gene (TATA-binding protein, *TBP*). The primers used are as follows: *Fak* (Fwd 5′-CCATGCCCTCGAAAAGCTATG; Rev 5′-TCCAATACAGCGT CCAAGTTCTA), *Pyk2* (Fwd 5′-CAGCAGAAGCAGATGGTGGA; Rev 5′-CC CTGTGAACTCCGTGTAGC), and *TBP* (Fwd 5′-GAAGCTGCGGTACAA TTCCAG; Rev 5′-CCCCTTGTACCCTTCACCAAT).

Drugs and peptides

The dual FAK/PYK2 inhibitor, PF-431396 (PF, Tocris Bioscience, Bristol, UK), was dissolved in sterile dimethyl sulfoxide (DMSO, Sigma-Aldrich, St. Louis, MO). Recombinant mouse leptin was from A. F. Parlow (National Hormone and Peptide Program, Torrance, CA) and Sigma-Aldrich (#L3772, St. Louis, MO) and was dissolved in sterile phosphate-buffered saline (PBS, Thermo Fisher Scientific, Waltham, MA) or sterile 20 mM Tris/HCl, pH 8.0. The angiotensin II (Sigma-Aldrich, St. Louis, MO) was dissolved in PBS. Tubastatin A Hydrochloride (MCE, Medchem Express) was dissolved in 20% DMSO/30% PBS/50% polyethylene glycol (PEG)-400 (Sigma-Aldrich).

Immunoprecipitation and immunoblotting

Cell plates for immunoblot analysis were removed from −80 °C and briefly thawed on ice prior to addition of RIPA buffer (50 mM TRIS pH: 7.50, 25 mM NaF, 100 mM NaCl, 5 mM EDTA, 0.1% SDS, 1% TritonX-100) supplemented with protease (complete EDTA-free protease inhibitor tablets, Roche, Basel, Switzerland) and phosphatase inhibitors (PhosSTOP phosphatase inhibitor tablets, Roche, Basel, Switzerland). For immunoprecipitation experiments, cells were washed one time with ice-cold PBS prior to addition of RIPA buffer without SDS (50 mM TRIS pH:7.50, 25 mM NaF, 100 mM NaCl, 5 mM EDTA, 1% TritonX-100) supplemented with protease and phosphatase inhibitors. Cells lysates were gently agitated for 15 min at 4 °C prior to centrifugation at 17,000 × *g* for 10 min at 4 °C. Total protein concentration of the cleared lysates were quantified using the Pierce BCA Protein Assay Kit (Thermo Fisher Scientific, Waltham, MA) according to the manufacturer's protocol. Immunoprecipitation was carried out overnight at 4 °C using 1 μg antibody per mg protein in the lysate. The immunoprecipitation experiments using hypothalamic lysates were carried out after crosslinking freshly dissected tissues in 10% formalin for 30 min at 4 °C. Tissues were next treated with glycine for 30 min, and then homogenized in RIPA buffer as described above. Cleared lysates were incubated with STAT3 or IgG antibodies for immunoprecipitation. Protein A/G beads were added for another 2 h, and the beads were washed 3 times with RIPA buffer and bound proteins were eluted in 2x laemmli buffer. Lysates were briefly boiled for 3–4 min, except for when blotting for LepRb, prior to being loaded on an SDS-PAGE gel (BioRad, Hercules, CA). Electrophoresed proteins were transferred to a PVDF membrane (Millipore, Burlington, MA). After transfer, membranes were blocked in a solution of bovine serum albumin (Research Products International, Mount Prospect, IL) in PBS prior to incubation with indicated primary antibodies for 1 h at room temperature or overnight at 4 °C. Blots were washed with PBST (PBS with 0.1% Tween-20) for 30 min. Blots were then incubated with an HRP- or a fluorophore-conjugated secondary antibody for 1 h at room temperature followed by washing for 30 min with PBST. Blots were developed immediately following the first 30 min wash. Blots incubated with an HRP-conjugated secondary antibody were developed using West Femto ECL Substrate (Thermo Fisher Scientific, Waltham, MA) and visualized using a Bio-Rad ChemiDoc Touch Imaging System (BioRad, Hercules, CA). Blots incubated with a fluorophore-conjugated secondary antibody were visualized using an Odyssey CLx imager (LI-COR Biosciences, Lincoln, NE). Some membranes were incubated at 37 °C in stripping buffer (Thermo Fisher Scientific, Waltham, MA) for 1 h prior to re-blocking and re-probing the membrane with another antibody. A relevant molecular weight marker is labeled in each immunoblot.

Immunoblot quantification

ImageJ (https://imagej.nih.gov/) was used for all immunoblot quantifications. To calculate the relative leptin induced pSTAT3/STAT3 values, each quantified pSTAT3 band was normalized to the quantified total STAT3 band. Then, each sample was normalized to the average of the unstimulated control sample(s).

RNAScope and microscopy

RNAScope fluorescent in situ hybridization. To quantify *Ptk2, Ptk2b* and *Lepr* mRNA abundance in the hypothalamus, RNAScope fluorescent multiplex v2 assay (Advanced Cell Diagnostics) was used. Fresh brain samples were collected from ad lib fed, overnight fasted, and leptin-treated fasted mice. Following dissection, brain samples were embedded in OCT and immediately frozen on dry ice and stored at −80 °C until further processing. A total of 16 μm-thick frozen sections covering the hypothalamus were cryostat sectioned and mounted onto Super Frost Plus slides (Fisher Scientific). In situ hybridization was performed according to the RNAscope fluorescent v2 multiplex kit user manual for fresh frozen tissue (Advanced Cell Diagnostics), using RNAscope Probe-Mm-Ptk2-C1(#511721), RNAscope Probe-Mm-Ob-r-C2(#402731-C2), and RNAscope Probe-Mm-Ptk2b-C3 (#506861-C3).

Image capture. Confocal Z-stacks comprised of 1.0-μm optical sections through triple-labeled sections were captured at ×20 magnification using a Leica SP8 confocal laser scanning system attached to a motorized inverted microscope (Leica Microsystems). Fluorophores were detected by four lasers at wavelengths of 405, 488, 561, and 640 nm.

Analysis of mRNA transcripts. Cells in each area (DMH, VMH, and ARH) were analyzed using Leica LAS X Life Science Microscope Software (Leica Microsystems). A fixed threshold and uniform roi was applied to all images, but separately for each channel and for each nucleus. Pixels above background were measured in optical sections through the entirety of each cell (indicated by a defined nucleus) and averaged per cell, to calculate animal averages and group means.

Co-localization analysis of transcripts. To examine whether there was a difference in the percentage of co-expression of *LepR*/*Pyk2*/*Fak* transcripts within a nucleus, images were taken on a Leica SP8 confocal laser scanning system at ×20 magnification. The total number of cells expressing either *LepR*, *Pyk2* and/or *Fak* was counted in sections of the DMH, VMH and ARH for each group, and the mean percentage of triple-labeled (*LepR*+*Pyk2*+*Fak*), double-labeled (*LepR*+*Pyk2*, *LepR*+*Fak*, or *Pyk2*+*Fak*), or single-labeled (*LepR*, *Pyk2*, or *Fak*) cells was calculated.

Single-cell RNA sequencing analysis

Processed single-cell RNA sequencing data of the hypothalamus[57] was downloaded from GEO (GSE87544). All analyses were conducted using the R package Seurat (v.4.3.0)[74,75]. The raw reads from 14,437 hypothalamic single cells were normalized and scaled. Top 2000 highly variable genes were identified and used as input for principal component analysis. Top 15 principal components (PCs) were determined to capture the greatest variance using the ElbowPlot function, and were used as input for the clustering analysis (resolution of 0.1) which was visualized with UMAP. Robustness of the clustering was evaluated by varying the PC and resolution parameters. The expression pattern of features of interest was evaluated using the FeaturePlot function. The scripts used to perform the scRNA sequencing analysis are available in Supplementary Note 1.

Statistics and reproducibility

All data are presented as the mean ± standard error of the mean (SEM) with a p value < 0.05 considered statistically significant. Unpaired and two-tailed t-test and one- and two-way ANOVA followed by Tukey's or Sidak multiple comparison test were applied. For N1Stat3Luc analysis (Fig. 3j, k), following transformation of the data, a nonlinear regression was used. All statistical analyses were conducted using GraphPad Prism (GraphPad, La Jolla, CA). p values are indicated in the figures. Sample sizes are indicated in figure legends. No statistical method was used to predetermine sample size. For the studies that involve stereotaxic surgeries into the lateral ventricle, the animals that tested negative during the water intake test (Angiotensin II test) were excluded from the study. Mice that were transduced with AAV particles were analyzed after the completion of the experiments and negatively targeted animals were excluded from the post hoc analysis. Allocation of samples or animals were random. The Investigators were not blinded to allocation during experiments and outcome assessment except for the experiments presented in Figs. 4, 5c and Supplementary Figs. 4, 5.

Reporting summary

Further information on research design is available in the Nature Portfolio Reporting Summary linked to this article.

Data availability

All data are contained within this article and in the Supporting Information. GSE96627[76], GSE68177[58], GSE124693[59], and GSE87544[57] are publicly available and used for re-analysis in our study. The hypothalamic RNAseq results of vehicle versus TubA-treated mice using in Fig. 1 is available at the sequence read archive with the BioProject ID: PRJNA1392032. Source data are provided with this paper.

References

1. Tang-Christensen, M., Havel, P. J., Jacobs, R. R., Larsen, P. J. & Cameron, J. L. Central administration of leptin inhibits food intake and activates the sympathetic nervous system in rhesus macaques. *J. Clin. Endocrinol. Metab.* **84**, 711–717 (1999).
2. Campfield, L. A., Smith, F. J., Guisez, Y., Devos, R. & Burn, P. Recombinant mouse OB protein: evidence for a peripheral signal linking adiposity and central neural networks. *Science* **269**, 546–549 (1995).
3. Coleman, D. L. Obese and diabetes: two mutant genes causing diabetes-obesity syndromes in mice. *Diabetologia* **14**, 141–148 (1978).
4. Strobel, A., Issad, T., Camoin, L., Ozata, M. & Strosberg, A. D. A leptin missense mutation associated with hypogonadism and morbid obesity. *Nat. Genet.* **18**, 213–215 (1998).
5. Elmquist, J. K., Bjørbaek, C., Ahima, R. S., Flier, J. S. & Saper, C. B. Distributions of leptin receptor mRNA isoforms in the rat brain. *J. Comp. Neurol.* **395**, 535–547 (1998).
6. Cohen, P. et al. Selective deletion of leptin receptor in neurons leads to obesity. *J. Clin. Invest.* **108**, 1113–1121 (2001).
7. Bates, S. H. et al. STAT3 signalling is required for leptin regulation of energy balance but not reproduction. *Nature* **421**, 856–859 (2003).
8. Pan, W. et al. Transcriptional and physiological roles for STAT proteins in leptin action. *Mol Metab* **22**, 121–131 (2019).
9. Piper, M. L., Unger, E. K., Myers, M. G. Jr & Xu, A. W. Specific physiological roles for signal transducer and activator of transcription 3 in leptin receptor-expressing neurons. *Mol. Endocrinol.* **22**, 751–759 (2008).
10. Jiang, L., Li, Z. & Rui, L. Leptin stimulates both JAK2-dependent and JAK2-independent signaling pathways. *J. Biol. Chem.* **283**, 28066–28073 (2008).
11. Wu, Z. et al. Integrin αVβ1-activated PYK2 promotes the progression of non-small-cell lung cancer via the STAT3-VGF axis. *Cell Commun. Signal.* **22**, 313 (2024).
12. Meads, M. B. et al. Targeting PYK2 mediates microenvironment-specific cell death in multiple myeloma. *Oncogene* **35**, 2723–2734 (2016).
13. Banerjee, K. et al. Reduced FAK-STAT3 signaling contributes to ER stress-induced mitochondrial dysfunction and death in endothelial cells. *Cell. Signal.* **36**, 154–162 (2017).
14. Avraham, H., Park, S. Y., Schinkmann, K. & Avraham, S. RAFTK/Pyk2-mediated cellular signalling. *Cell. Signal.* **12**, 123–133 (2000).
15. Guidetti, G. F., Torti, M. & Canobbio, I. Focal adhesion kinases in platelet function and thrombosis. *Arterioscler. Thromb. Vasc. Biol.* **39**, 857–868 (2019).
16. Schaller, M. D. Cellular functions of FAK kinases: insight into molecular mechanisms and novel functions. *J. Cell Sci.* **123**, 1007–1013 (2010).
17. Avraham, S. et al. Identification and characterization of a novel related adhesion focal tyrosine kinase (RAFTK) from megakaryocytes and brain. *J. Biol. Chem.* **270**, 27742–27751 (1995).
18. Schlaepfer, D. D., Hauck, C. R. & Sieg, D. J. Signaling through focal adhesion kinase. *Prog. Biophys. Mol. Biol.* **71**, 435–478 (1999).
19. Okigaki, M. et al. Pyk2 regulates multiple signaling events crucial for macrophage morphology and migration. *Proc. Natl. Acad. Sci. USA* **100**, 10740–10745 (2003).
20. Ilić, D. et al. Reduced cell motility and enhanced focal adhesion contact formation in cells from FAK-deficient mice. *Nature* **377**, 539–544 (1995).
21. Furuta, Y. et al. Mesodermal defect in late phase of gastrulation by a targeted mutation of focal adhesion kinase, FAK. *Oncogene* **11**, 1989–1995 (1995).
22. Lipinski, C. A. & Loftus, J. C. Targeting Pyk2 for therapeutic intervention. *Expert Opin. Ther. Targets* **14**, 95–108 (2010).
23. Lim, Y. et al. PyK2 and FAK connections to p190Rho guanine nucleotide exchange factor regulate RhoA activity, focal adhesion formation, and cell motility. *J. Cell Biol.* **180**, 187–203 (2008).
24. Sieg, D. J. et al. Pyk2 and Src-family protein-tyrosine kinases compensate for the loss of FAK in fibronectin-stimulated signaling events but Pyk2 does not fully function to enhance FAK- cell migration. *EMBO J.* **17**, 5933–5947 (1998).
25. Weis, S. M. et al. Compensatory role for Pyk2 during angiogenesis in adult mice lacking endothelial cell FAK. *J. Cell Biol.* **181**, 43–50 (2008).

26. Canobbio, I. et al. Impaired thrombin-induced platelet activation and thrombus formation in mice lacking the Ca(2+)-dependent tyrosine kinase Pyk2. *Blood* **121**, 648–657 (2013).
27. Canobbio, I. et al. The focal adhesion kinase Pyk2 links Ca2+ signalling to Src family kinase activation and protein tyrosine phosphorylation in thrombin-stimulated platelets. *Biochem. J.* **469**, 199–210 (2015).
28. Kornberg, L., Earp, H. S., Parsons, J. T., Schaller, M. & Juliano, R. L. Cell adhesion or integrin clustering increases phosphorylation of a focal adhesion-associated tyrosine kinase. *J. Biol. Chem.* **267**, 23439–23442 (1992).
29. Guan, J. L., Trevithick, J. E. & Hynes, R. O. Fibronectin/integrin interaction induces tyrosine phosphorylation of a 120-kDa protein. *Cell Regul.* **2**, 951–964 (1991).
30. Astier, A., Avraham, H., Manie, S. N. & Groopman, J. The related adhesion focal tyrosine kinase is tyrosine-phosphorylated after β1-integrin stimulation in B cells and binds to p130cas. *J. Biol. Chem.* **272**, 228–232 (1997).
31. Li, J., Avraham, H., Rogers, R. A., Raja, S. & Avraham, S. Characterization of RAFTK, a novel focal adhesion kinase, and its integrin-dependent phosphorylation and activation in megakaryocytes. *Blood* **88**, 417–428 (1996).
32. Robles, E. & Gomez, T. M. Focal adhesion kinase signaling at sites of integrin-mediated adhesion controls axon pathfinding. *Nat. Neurosci.* **9**, 1274–1283 (2006).
33. Shi, Y., Pontrello, C. G., DeFea, K. A., Reichardt, L. F. & Ethell, I. M. Focal adhesion kinase acts downstream of EphB receptors to maintain mature dendritic spines by regulating cofilin activity. *J. Neurosci.* **29**, 8129–8142 (2009).
34. Giralt, A. et al. Pyk2 modulates hippocampal excitatory synapses and contributes to cognitive deficits in a Huntington's disease model. *Nat. Commun.* **8**, 15592 (2017).
35. Mastrolia, V., Al Massadi, O., de Pins, B. & Girault, J.-A. Pyk2 in dorsal hippocampus plays a selective role in spatial memory and synaptic plasticity. *Sci. Rep.* **11**, 16357 (2021).
36. Shi, C.-S. & Kehrl, J. H. Pyk2 amplifies epidermal growth factor and c-Src-induced Stat3 activation. *J. Biol. Chem.* **279**, 17224–17231 (2004).
37. Murphy, J. M. et al. FAK and Pyk2 activity promote TNF-alpha and IL-1beta-mediated pro-inflammatory gene expression and vascular inflammation. *Sci. Rep.* **9**, 7617 (2019).
38. Selitrennik, M. & Lev, S. PYK2 integrates growth factor and cytokine receptors signaling and potentiates breast cancer invasion via a positive feedback loop. *Oncotarget* **6**, 22214–22226 (2015).
39. Canino, J. et al. The proline-rich tyrosine kinase Pyk2 modulates integrin-mediated neutrophil adhesion and reactive oxygen species generation. *Biochim. Biophys. Acta Mol. Cell Res.* **1867**, 118799 (2020).
40. Bisht, B., Srinivasan, K. & Dey, C. S. In vivo inhibition of focal adhesion kinase causes insulin resistance. *J. Physiol.* **586**, 3825–3837 (2008).
41. Luk, C. T. et al. FAK signalling controls insulin sensitivity through regulation of adipocyte survival. *Nat. Commun.* **8**, 14360 (2017).
42. Yu, Y. et al. Role of PYK2 in the development of obesity and insulin resistance. *Biochem. Biophys. Res. Commun.* **334**, 1085–1091 (2005).
43. Andreoli, M. F., Donato, J., Cakir, I. & Perello, M. Leptin resensitisation: a reversion of leptin-resistant states. *J. Endocrinol.* **241**, R81–R96 (2019).
44. Çakır, I. et al. Histone deacetylase 6 inhibition restores leptin sensitivity and reduces obesity. *Nat. Metab.* **4**, 44–59 (2022).
45. Ahima, R. S. HDAC6 inhibition overcomes leptin resistance in obesity. *Nat. Metab.* **4**, 11–12 (2022).
46. Allison, M. B. et al. Defining the transcriptional targets of leptin reveals a role for Atf3 in leptin action. *Diabetes* https://doi.org/10.2337/db17-1395 (2018).
47. Dornbos, P. et al. Evaluating human genetic support for hypothesized metabolic disease genes. *Cell Metab.* **34**, 661–666 (2022).
48. Costanzo, M. C. et al. The Type 2 Diabetes Knowledge Portal: an open access genetic resource dedicated to type 2 diabetes and related traits. *Cell Metab.* **35**, 695–710.e6 (2023).
49. Han, S. et al. Structural characterization of proline-rich tyrosine kinase 2 (PYK2) reveals a unique (DFG-out) conformation and enables inhibitor design. *J. Biol. Chem.* **284**, 13193–13201 (2009).
50. Parganas, E. et al. Jak2 is essential for signaling through a variety of cytokine receptors. *Cell* **93**, 385–395 (1998).
51. Kohlhuber, F. et al. A JAK1/JAK2 chimera can sustain alpha and gamma interferon responses. *Mol. Cell. Biol.* **17**, 695–706 (1997).
52. Burfoot, M. S. et al. Janus kinase-dependent activation of insulin receptor substrate 1 in response to interleukin-4, oncostatin M, and the interferons. *J. Biol. Chem.* **272**, 24183–24190 (1997).
53. Choi, S. K., Park, S. & Moon, H.-S. Nuclear translocation of STAT3 by in vitro metreleptin administration causes lipolysis in human primary adipocytes. *Braz. Arch. Biol. Technol.* **59**, e16150605 (2016).
54. Moon, H.-S., Chamberland, J. P. & Mantzoros, C. S. Amylin and leptin activate overlapping signalling pathways in an additive manner in mouse GT1-7 hypothalamic, C2C12 muscle and AML12 liver cell lines. *Diabetologia* **55**, 215–225 (2012).
55. Han, C., Wu, W., Ale, A., Kim, M. S. & Cai, D. Central leptin and tumor necrosis factor-α (TNFα) in diurnal control of blood pressure and hypertension. *J. Biol. Chem.* **291**, 15131–15142 (2016).
56. Silver, D. L., Naora, H., Liu, J., Cheng, W. & Montell, D. J. Activated signal transducer and activator of transcription (STAT) 3: localization in focal adhesions and function in ovarian cancer cell motility. *Cancer Res.* **64**, 3550–3558 (2004).
57. Chen, R., Wu, X., Jiang, L. & Zhang, Y. Single-cell RNA-seq reveals hypothalamic cell diversity. *Cell Rep.* **18**, 3227–3241 (2017).
58. Henry, F. E., Sugino, K., Tozer, A., Branco, T. & Sternson, S. M. Cell type-specific transcriptomics of hypothalamic energy-sensing neuron responses to weight-loss. *Elife* **4**, e09800 (2015).
59. Cedernaes, J. et al. Transcriptional basis for rhythmic control of hunger and metabolism within the AgRP neuron. *Cell Metab.* **29**, 1078–1091.e5 (2019).
60. Greenhill, C. A role for HDAC6 in leptin sensitivity. *Nat. Rev. Endocrinol.* **18**, 194 (2022).
61. Fan, H. & Guan, J.-L. Compensatory function of Pyk2 protein in the promotion of focal adhesion kinase (FAK)-null mammary cancer stem cell tumorigenicity and metastatic activity. *J. Biol. Chem.* **286**, 18573–18582 (2011).
62. Monje, F. J. et al. Focal adhesion kinase regulates neuronal growth, synaptic plasticity and hippocampus-dependent spatial learning and memory. *Neurosignals* **20**, 1–14 (2012).
63. Bouret, S. G., Draper, S. J. & Simerly, R. B. Trophic action of leptin on hypothalamic neurons that regulate feeding. *Science* **304**, 108–110 (2004).
64. Guan, D. et al. Central inhibition of HDAC6 re-sensitizes leptin signaling during obesity to induce profound weight loss. *Cell Metab.* **36**, 857–876.e10 (2024).
65. Xu, J. et al. Genetic identification of leptin neural circuits in energy and glucose homeostases. *Nature* **556**, 505–509 (2018).
66. Tan, H. L. et al. Leptin-activated hypothalamic BNC2 neurons acutely suppress food intake. *Nature* **636**, 198–205 (2024).
67. Webster, A. N. et al. Molecular connectomics reveals a glucagon-like peptide 1-sensitive neural circuit for satiety. *Nat. Metab.* **6**, 2354–2373 (2024).
68. Zhu, C. et al. Profound and redundant functions of arcuate neurons in obesity development. *Nat. Metab.* **2**, 763–774 (2020).

69. Hill, J. W. et al. Acute effects of leptin require PI3K signaling in hypothalamic proopiomelanocortin neurons in mice. *J. Clin. Invest.* **118**, 1796–1805 (2008).
70. Ghilardi, N. & Skoda, R. C. The leptin receptor activates janus kinase 2 and signals for proliferation in a factor-dependent cell line. *Mol. Endocrinol.* **11**, 393–399 (1997).
71. Baumann, H. et al. The full-length leptin receptor has signaling capabilities of interleukin 6-type cytokine receptors. *Proc. Natl. Acad. Sci. USA* **93**, 8374–8378 (1996).
72. Ghilardi, N. et al. Defective STAT signaling by the leptin receptor in diabetic mice. *Proc. Natl. Acad. Sci. USA* **93**, 6231–6235 (1996).
73. Bjørbæk, C. et al. Divergent roles of SHP-2 in ERK activation by leptin receptors. *J. Biol. Chem.* **276**, 4747–4755 (2001).
74. Butler, A., Hoffman, P., Smibert, P., Papalexi, E. & Satija, R. Integrating single-cell transcriptomic data across different conditions, technologies, and species. *Nat. Biotechnol.* **36**, 411–420 (2018).
75. Stuart, T. et al. Comprehensive integration of single-cell data. *Cell* **177**, 1888–1902.e21 (2019).
76. Larder, R. et al. Obesity-associated gene TMEM18 has a role in the central control of appetite and body weight regulation. *Proc. Natl. Acad. Sci. USA* **114**, 9421–9426 (2017).

Acknowledgements

This work was supported by National Institutes of Health (NIH) R01DK070332 and 1R01DK125830 to Roger Cone, MDRC Pilot and Feasibility Grant (NIH grant P30-DK020572), the Klatskin–Sutker Discovery Fund, and the American Diabetes Association grant no. 7-21-JDF-032 to I.C., LSA Honors Summer Fellowship to C.K.H., and by the Italian Ministry of Education, University and Research (MIUR): Dipartimenti di Eccellenza Program (2018–2022)—Department of Biology and Biotechnology "L. Spallanzani", University of Pavia to L.G. C.K.H. was supported by a Medical Scientist Training Program grant from the National Institute of General Medical Sciences of the National Institutes of Health under award number: T32GM152349 to the Weill Cornell/Rockefeller/Sloan Kettering Tri-Institutional MD-PhD Program. The co-first authors contributed equally to this manuscript and support each co-first author listing their name in any order for the purposes of their professional records (e.g., CVs, résumés).

Author contributions

C.K.H., L.G., M.T., and I.C. conceived and designed the study. C.K.H., L.G., Y.G., D.T.P., A.M.C.S., Y.W., Y.L., and I.C. performed the experiments. All authors analyzed the data. C.K.H., L.G., and I.C. wrote the manuscript.

Competing interests

I.C. is an inventor on a provisional patent application on non-hydroxamate HDAC6 blockers. Other authors declare no competing interests.

Additional information

Supplementary information The online version contains supplementary material available at https://doi.org/10.1038/s41467-026-69008-9.

Correspondence and requests for materials should be addressed to Işın Çakır.

Peer review information *Nature Communications* thanks the anonymous reviewer(s) for their contribution to the peer review of this work. A peer review file is available.

Reprints and permissions information is available at http://www.nature.com/reprints

Publisher's note Springer Nature remains neutral with regard to jurisdictional claims in published maps and institutional affiliations.

Open Access This article is licensed under a Creative Commons Attribution-NonCommercial-NoDerivatives 4.0 International License, which permits any non-commercial use, sharing, distribution and reproduction in any medium or format, as long as you give appropriate credit to the original author(s) and the source, provide a link to the Creative Commons licence, and indicate if you modified the licensed material. You do not have permission under this licence to share adapted material derived from this article or parts of it. The images or other third party material in this article are included in the article's Creative Commons licence, unless indicated otherwise in a credit line to the material. If material is not included in the article's Creative Commons licence and your intended use is not permitted by statutory regulation or exceeds the permitted use, you will need to obtain permission directly from the copyright holder. To view a copy of this licence, visit http://creativecommons.org/licenses/by-nc-nd/4.0/.

© The Author(s) 2026